The Navigation Potential of Ground Feature Tracking

THESIS

Güner Mutlu, Captain, TUAF

AFIT/GE/ENG/09-52

DEPARTMENT OF THE AIR FORCE
AIR UNIVERSITY

AIR FORCE INSTITUTE OF TECHNOLOGY

Wright-Patterson Air Force Base, Ohio

The views expressed in this thesis are those of the author and do not reflect the official policy or position of the United States Air Force, Department of Defense, or the United States Government.

AFIT/GE/ENG/09-52

The Navigation Potential of Ground Feature Tracking

THESIS

Presented to the Faculty

Department of Electrical and Computer Engineering

Graduate School of Engineering and Management

Air Force Institute of Technology

Air University

Air Education and Training Command

In Partial Fulfillment of the Requirements for the

Degree of Master of Science (Electrical Engineering)

Güner Mutlu, B.S.

Captain, TUAF

September 2009

AFIT/GE/ENG/09-52

The Navigation Potential of Ground Feature Tracking

Güner Mutlu, B.S.
Captain, TUAF

Approved:

/signed/	Aug 2009
Dr.Meir Pachter, PhD (Chairman)	date
/signed/	Aug 2009
Dr. David Jacques (Member)	date
/signed/	Aug 2009
Lt.Col Michael Veth (Member)	date

AFIT/GE/ENG/09-52

Abstract

This research effort examines the reduction of error in inertial navigation aided by vision. This is part of an effort focused on navigation in a GPS denied environment. The navigation concept examined here consists of two main steps. First, extract the position of a tracked ground object using vision and geo-locate it in 3 dimensional navigation frame. In this first step multiple positions of the UAV are assumed known; think of a synthetic aperture. The only information about the tracked ground object-s/features is the unit vector that points to the objects from the center of the camera. Two such vectors give enough information to calculate the best estimate of the position of the tracked object in a 3 dimensional navigation frame using the method of least square. Concerning the second step: checking observability for the 3-D case shows that at least 2 objects need to be tracked. In practice one needs to track more than two objects to wash out the measurement error and obtain good results.

In the first step the known position of the UAV is used to first geo-locate the tracked ground object while relaying on the short time span accuracy of the INS. In the second step, the information on the position of multiple tracked objects is used as points of origin of vectors that point to the UAV, instead of using multiple positions of the air vehicle, as was the done in step one. The least squares method is applied to determine the position of the UAV. As explained above, initially using known positions, of the air vehicle, the positions of the tracked ground objects are calculated, and then using those calculated positions the position of the UAV is determined. These two steps feed each other.

The performance of the Kalman filter and UAV position estimation algorithms strongly depend on the quality of the measurements provided by the INS. The INS measure-

ments were modeled, and we investigated simplified flying scenarios to validate our algorithms/methodology.

Some effort was expanded on investigating the possibility of using a camera and GPS position measurements,without using INS. Directly using the Doppler readings provided by GPS might be advantageous.

The investigated scenarios showed that bearings measurements of ground objects taken over time are useful for enhancing the INS navigation solution. When multiple objects are tracked, the algorithm is applied to each pair of objects and the results were averaged. This method gave us better results and at the same time is somewhat more practical than extending the algorithm to accommodate an arbitrary number of tracked objects.

Acknowledgements

I would like to thank to Dr.Pachter for his contribution and his diligent support and encouragement to me for producing this thesis. I also want to thank to him for letting me to have benefits from his great experience.

I want to thank to Lt.Col.Veth for teaching me invaluable classes, and for being always helpful to all his students. I need to say how I am impressed to see his hard work to prepare material for us, and attempt to update his teaching methods.

I greatly appreciate to Dr.Jacques for letting me to have benefits from his great experience and vision, for his comments about my thesis, and for his invaluable advices related to my dual degree.

i also owe thanks to Maj.Saville for his help to schedule my two years upfront, and to help me to be able to take all classes on time for my dual degree program.

I also want to thank to my mom, who always provides me her love, and for her just on time visit that gave me the highest moral at the time when I needed at most.

Güner Mutlu

Table of Contents

List of Figures

List of Tables

List of Abbreviations

The Navigation Potential of Ground Feature Tracking

I. Introduction

1.1 Background

Navigation has a long history. Currently, commercial nav-aids like VOR (VHF Omni-directional Radio Range), NDB (Non-directional beacon), DME (Distance measuring equipment) work well and GPS (Global positioning system) provides very precise positioning, and it is widely used. In this thesis the use of vision for navigation is investigated for use in areas of conflict with perhaps reduced GPS availability, in order to guarantee more robust navigation.

Consider a target located thousands of miles away from the nearest safe base in a partner country; and assume the enemy is surrounded by neighboring countries which are not willing to provide logistic support to our operation. An UAV would be used in such an operation because not using personnel will save lives. The UAV should be able to take part in a global operation. In addition, a small UAV will be cheaper than a conventional jet fighter or bomber, and there is no need to use an Air Force installation close to the area of conflict. The operation can be started sooner and will cost less.

How can this be accomplished? The UAV can be launched safely from one of our Air Bases, and can fly on its route using conventional nav-aids without having any problems until approaching the area of conflict. In the battle zone it needs to be prepared to lose some nav-aid options. Autonomous vision-aided INS navigation will be helpful here. This is a passive navigation method that cannot be jammed by electromagnetic interference. Also, an IR camera could be used since it is less affected by humidity in the air or cloud. In the battle space, say an area of a hundred square miles, navigation will be accomplished by tracking ground features using an airborne

camera.

Furthermore, stationary ground objects, like trees, big rocks, buildings or other objects will be used to map the battle-zone. Our hunter UAV is a moving object, and other moving objects are possibly friends or enemies. The object tracking algorithm will calculate the relative position between stationary objects, the UAV and the target, and possibly other moving objects. Kalman filtering will be used.

1.2 Problem Statement for Level Flight and Maneuvers

During level flight the ground object should be continuously tracked. Using the known speed and altitude of the UAV the position of the tracked object in the next image can be predicted. This will narrow the search for locating the object/feature in the next frame. To not lose the update information, it's necessary to track four or five ground objects. It all depends on how good the real-time feature extraction algorithm is.

We note that tracked objects in the scene should not be arranged on one line. It's good to have the tracked objects spread out in the scene in every frame. The overlap of the objects' pattern in the scene will provide continuous update information and will be a good aid to INS.

Unfortunately flights, especially military flights, will not be only level flights. Military aircraft and even UAVs need to maneuver. Let's take a barrel roll as an example. A down looking camera will lose sight of the ground objects for a short time during upside-down flight. One should then map the last group of visible ground objects on a digital map of the 3 dimensional world around the UAV, and then calculate the predicted position of those objects until the time of recapturing of at least one ground object. Hence, to not lose the tracked objects a camera which has a wide angle lens such that it can capture a wide field of view is required.

In the case of a total loss of ground objects, forward propagation of the UAV's position might not be reliable. If we have a good GPS signal or update from other

sensors, sensor fusion will be helpful here to aid the INS. Especially for this case, mapping of the tracked objects in the 3D world and saving them in memory is very important; the combat zone could be an area less than 100 square miles and information about many ground objects could be stored in memory. Good $3-D$ maps of that area can be extracted and stored in memory like pieces of a huge puzzle. Flying a few times over the same area may help to fill out some gaps. It might not be imperative to fill all gaps in the battle space. We will need navigation information to get the job done and finally to exit the battle zone and return to base. Producing that kind of $3D$ map by filling gaps depends on really good feature tracking and good matching/image correspondence algorithms.

1.3 Scope

There is increased use of UAVs today. What requires increased numbers of sorties of UAVs in the battlefield? Increasing sensitivity of the public to lost personnel force leadership to look for methods to save life of troops. Using unmanned systems reduces risk to the crew.

There is always a need to reduce the cost. The cost of production and also the cost of maintenance. If you don't need to have a pilot in the cockpit, that means you will save weight and also here will be no need for systems designed to save his life. Here we can include input-output devices that help the pilot to communicate with the aircraft, and to control it. Many subsystems are needed for a human on board. Using an UAV will save weight and expenses related to those devices. Affordable war machines are always attractive to the leadership.

We need to add that pilot emergencies are not expected in UAVs. Are they eligible to replace all jet fighters or bombers? For now there is still need to use conventional weapon systems, however a lot of studies are done to improve the capabilities of unmanned systems in the air, on the ground and at sea.

What about requirement for invisibility in the battlefield? There are many different sensors available for navigation. Radar, ladar, laser altemeter etc... We need to be

able to use all options, even that we will not use all of them at the same time or at the same aircraft. Emitting sensors could be defined by the enemy, so that requires research to use passive sensors for navigation for some cases.
In this thesis the use of vision for navigation is investigated for use in areas of conflict with perhaps reduced GPS availability, in order to guarantee more robust navigation. Vision aid is passive and could be fully autonomous. Does not need help from satellite or other sources. It is not electronically jammable. Can replace some of other INS aid sensors.

1.4 Approach/Methodology

To document the research conducted in this thesis, each chapter will be briefly summarized. The first chapter some background information abut navigation, problem statement from hight point of view, brief information about Systems Engineering and Management and its principles, and finally summary of the whole document. The second chapter includes background information about INS and different types of frames used in navigation. Chapter three examines mathematical theory used in this thesis. This chapter first investigates 2-D flight scenario and related mathematics; then extends the theory and mathematics for 3-D flight scenario. Methods to go between frames are explained and applied for investigated flight scenario in this chapter. Time dependent state space representation needed for Kalman filtering was obtained in this section. Chapter four consists of simulations, results, and briefly information about assumptions for applied scenarios. Chapter five consists of conclusion of the job done here and recommendations for next iterations.

II. Literature Review

2.1 Inertial Navigation

The inertial navigation systems depend on mechanic laws derived by Newton. An inertial navigation system consist of a computer and a platform or module containing accelerometers and gyroscopes. Inclinometers are also sometimes used. The INS is initially provided with its position and velocity from another source (a human operator, a GPS receiver, etc.), and thereafter computes its own updated position and velocity by integrating information received from the inertial sensors. The advantage of an INS is that it requires no external information in order to determine its position, orientation, or velocity once it has been initialized.

An INS can autonomously detect a change in its geographic position (a move East or North, for example), a change in its velocity (speed and direction of movement), and a change in its orientation (rotation about an axis). It does this by measuring the linear and angular accelerations of the UAV. Since it requires no external reference (after initialization), it is immune to jamming and deception. Inertial-navigation systems are used in ground vehicles, aircraft, ships, submarines, and guided missiles.

Gyroscopes measure the angular velocity of the system in the inertial reference frame. By using the original orientation of the aircraft in the inertial reference frame as the initial condition and integrating the angular velocity, the system's current orientation is obtained at all times. This can be thought of as the ability of a blindfolded passenger in a car to feel the car turn left and right or tilt up and down as the car ascends or descends hills. Based on this information alone, he knows in what direction the car is leading but does not know how fast or slow it is moving, or whether it is sliding sideways.

Accelerometers measure the linear acceleration of the system in the inertial reference frame, but in directions that can only be measured relative to the moving system (since the accelerometers are affixed to the vehicle and rotate with the vehicle, but are not aware of their own orientation). This can be thought of as the ability of a

blindfolded passenger in a car to feel himself pressed back into his seat as the vehicle accelerates forward or pulled forward as it slows down; and feel himself pressed down into his seat as the vehicle speeds up a hill or rise up out of his seat as the car passes over the crest of a hill and begins to descend. Based on this information alone, he knows how the vehicle is moving relative to itself, that is, whether it is going forward, backward, left, right, up (toward the car's ceiling), or down (toward the car's floor) measured relative to the car, but not the direction relative to Earth, since he did not know what direction the car was facing relative to Earth when he felt the accelerations.

All inertial navigation systems suffer from "integration drift": small errors in the measurement of acceleration and angular velocity are integrated into progressively larger errors in velocity, which is compounded into still greater errors in position. Since the new position is calculated solely from the previous position, these errors are cumulative, increasing at a rate roughly proportional or, on even higher route to the time since the initial position was input. Therefore the INS position fix must be periodically corrected by input from some other type of navigation system.

2.2 Coordinate Systems

2.2.1 The Inertial reference frame. The location of the origin may be any reference point that is completely unaccelerated (inertial), and the orientation of the axes is usually irrelevant in most problems so long as they too are fixed with respect to inertial space. The origin of the inertial reference frame I is at the center of the Earth. The geometry is illustrated in Figure2.1

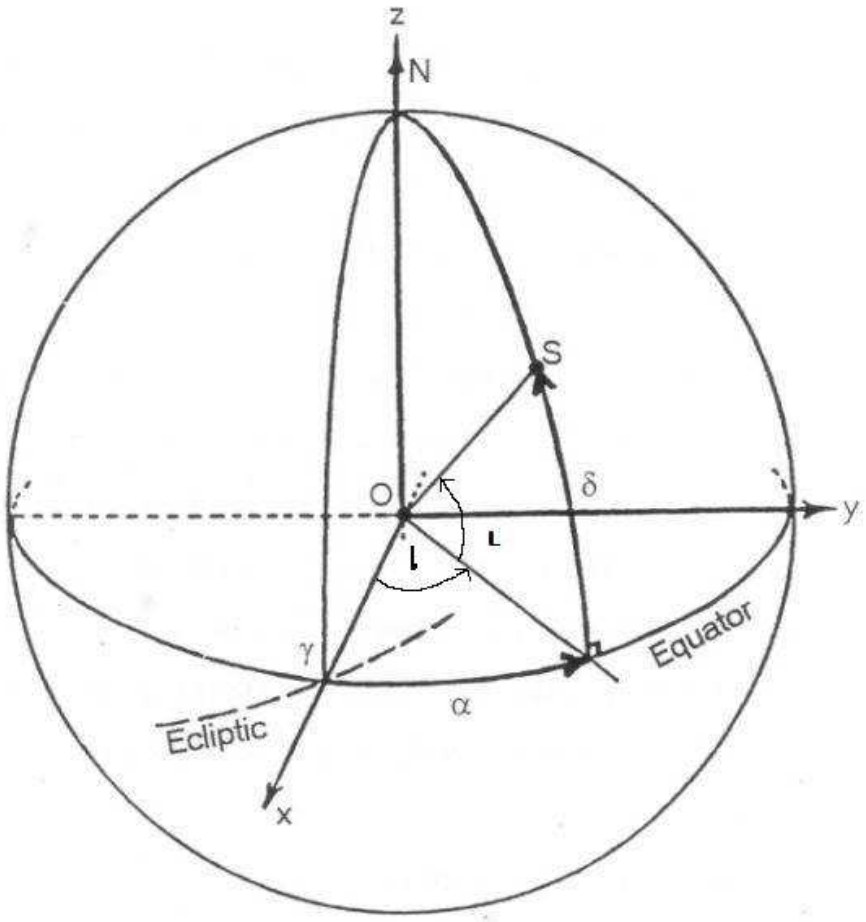

Figure 2.1: The Inertial reference frame

2.2.2 The Earth-Centered reference frame. As its name suggests this coordinate system has its origin at the center of the Earth. Its axes may be arbitrarily selected with respect to fixed positions on the surface of the Earth.This ECEF coordinate system obviously rotates with the Earth. The geometry is illustrated in

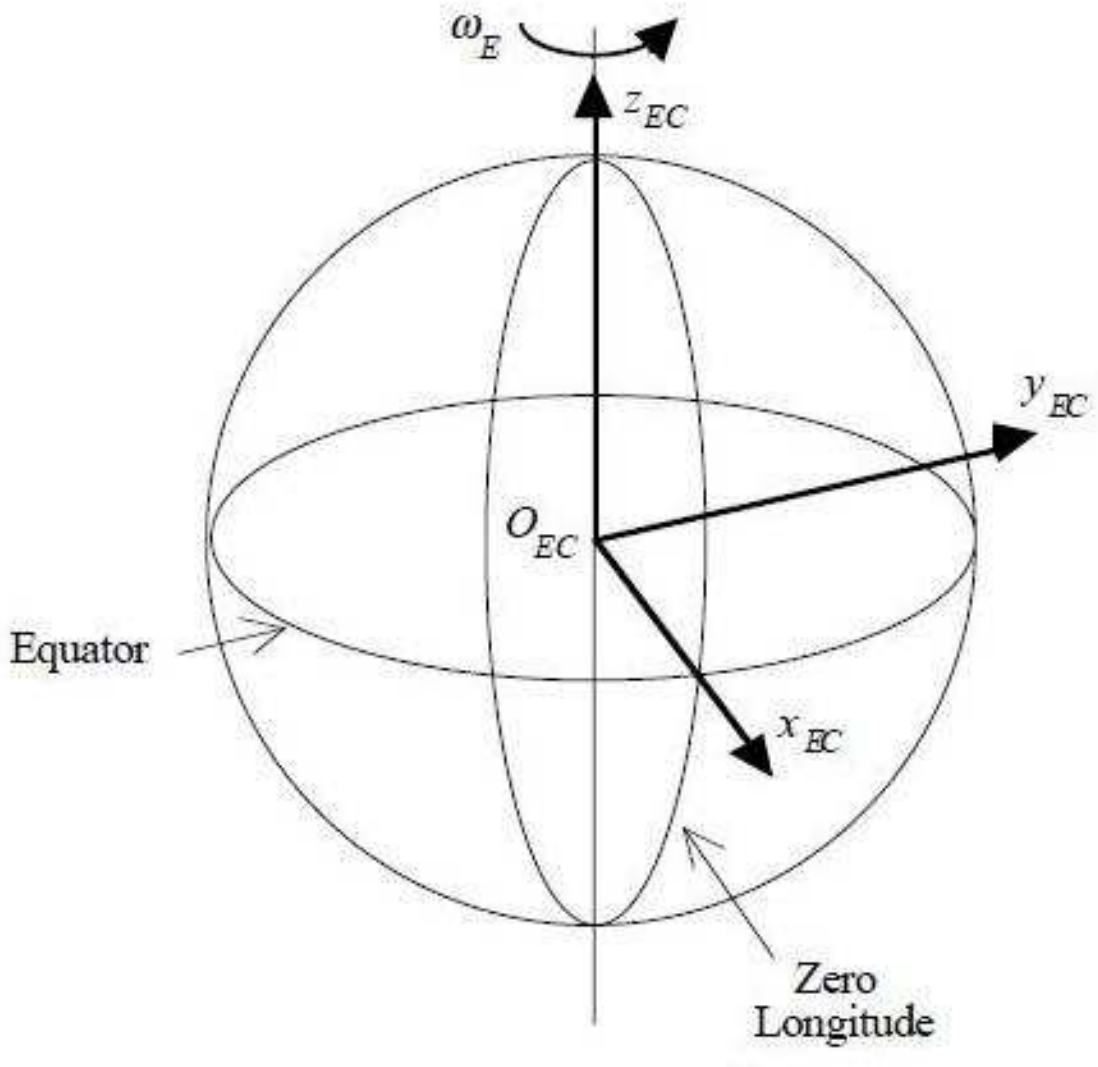

Figure 2.2: Earth-Centered Earth-Fixed reference frame ECEF

2.2.3 The Earth-fixed reference frame. This coordinate system has its origin fixed to an arbitrary point on the surface of the Earth. x_E points due North, y_E points due East, and z_E points toward the center of the Earth.

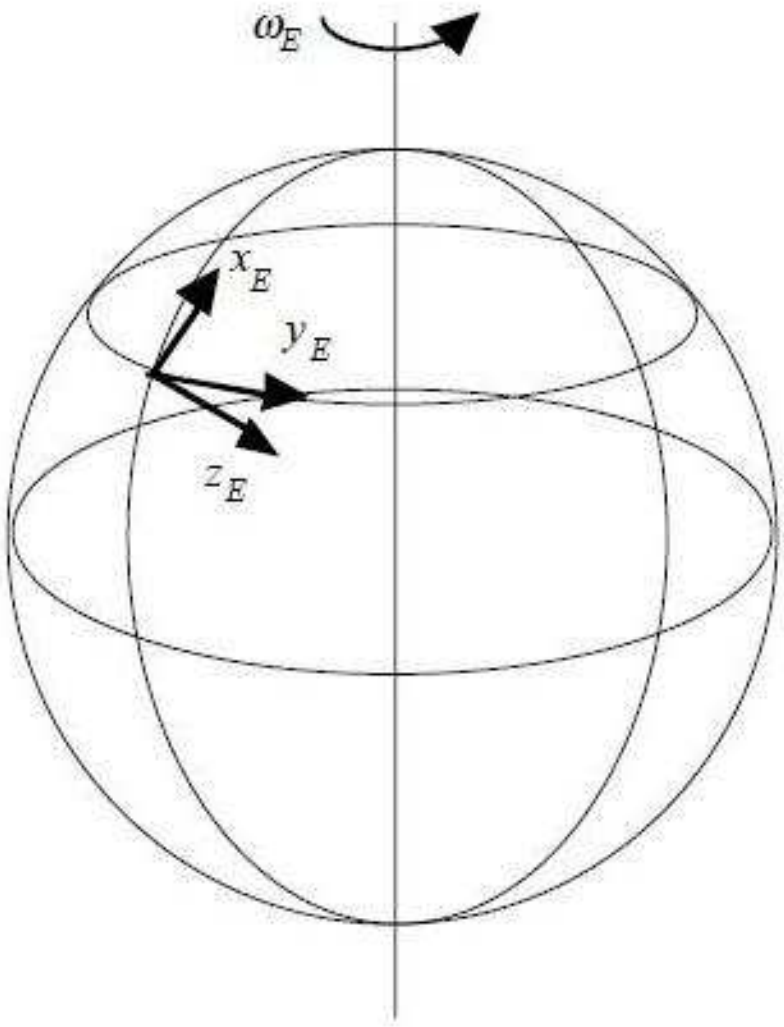

Figure 2.3: Earth-fixed reference frame

2.2.4 The Body-fixed frame. This coordinate system has its origin fixed to any arbitrary point that may be free to move relative to the Earth. For example, the origin may be fixed to the center of gravity (CG) of an aircraft and move with the

CG. y_N points due North, x_E points due East, and z_D points toward the center of the Earth.

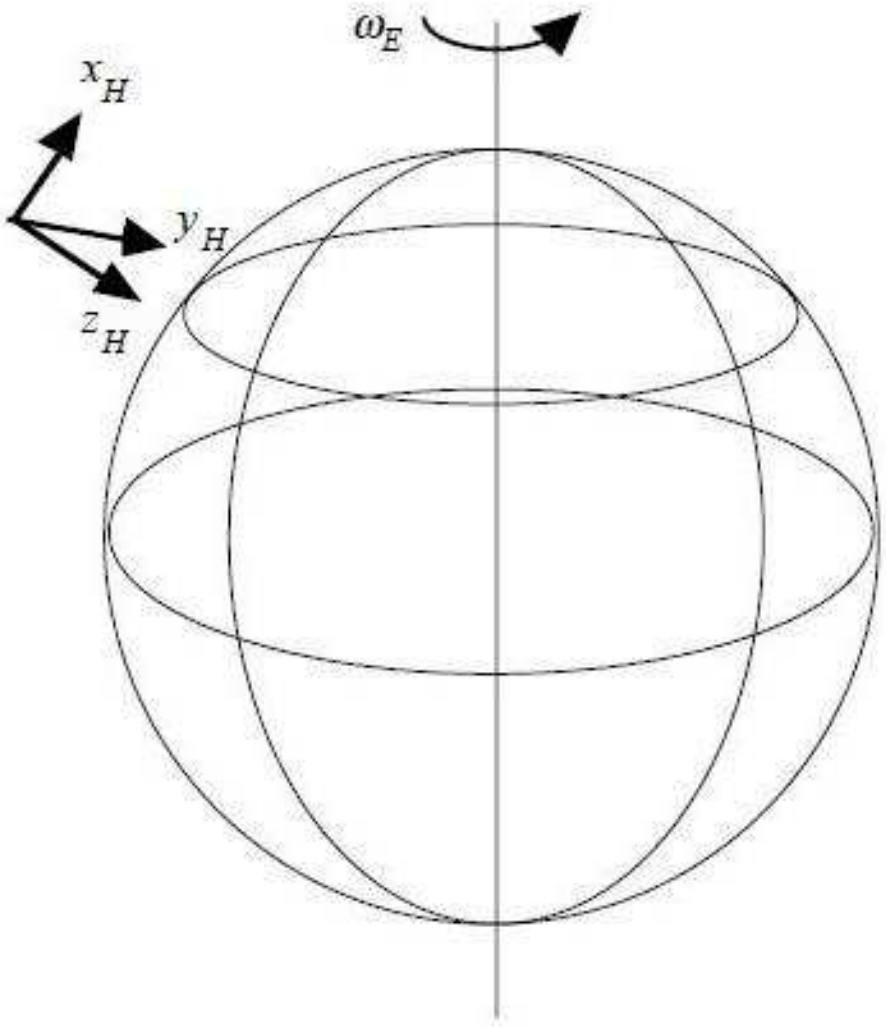

Figure 2.4: Body-fixed navigation reference frame

2.2.5 Body-fixed reference frames. "Body-fixed" means the origin and axes of the coordinate system are fixed with respect to the (nominal) geometry of the aircraft. This must be distinguished from body-carried systems in which the origin is fixed with respect to the body but the axes are free to rotate relative to it. In flight

dynamics reference frames are used which have their origin at the aircraft's CG and the x axis is aligned with the velocity vector and one then refers to the "wind axes".

Figure 2.5: Body-fixed reference frame shown on US Navy $F-14$ Tomcat

III. Methodology

3.1 Introduction

In this chapter we develop methods for visual INS aiding using optical measurements of tracked ground objects/ground features with known or unknown position. INS aiding using bearing measurements of stationary ground features is investigated. The objective is to quantify the navigation information obtained by tracking ground features over time. The answer is provided by an analysis of the attendant observability problem. The degree of INS aiding action is determined by the degree of observability provided by the measurement arrangement. The latter is strongly influenced by the nature of the available measurements - in our case, bearing measurements of stationary ground objects - the trajectory of the aircraft, and the length of the measurement interval. It is shown that when one known ground object is tracked, the observability Grammian is rank deficient and thus full INS aiding action is not available. However, if barometer altitude is available and an additional vertical gyroscope is used to provide an independent measurement of the aircraft's pitch angle, a data driven estimate of the complete navigation state can be obtained. If two ground features are simultaneously tracked the observability Grammian is full rank and all the components of the navigation state vector are positively impacted by the external measurements.

3.2 2-D Case

3.2.1 Introduction. Inertial Navigation System aiding using optical measurements [1–6] is appealing because passive bearing - only measurements preserve the autonomy of the integrated navigation system. In this thesis an attempt is made to gain an understanding of the nature of the navigation information provided by bearing - only measurements taken over time, of stationary ground objects, whose position is not necessarily known.

In this thesis the crucial issue of processing the images provided by a down looking camera for the autonomous - without human intervention - measurement of optic flow, or, alternatively, image correspondence for feature tracking, or, mosaicing, [7, 8] is not addressed. We do however note that these tasks are nevertheless somewhat easier than full blown Autonomous Target Recognition (ATR) and/or machine perception. In this article it is assumed that autonomous feature detection and tracking is possible so that bearings measurement records of stationary ground objects are available. We exclusively focus on gauging the navigation potential of bearings - only measurements of stationary ground objects taken over time.

In this thesis we refer to purely deterministic, i.e. noise free, corrupted bearing measurements, where many measurements would naturally help wash out the noise. Even so, both the number of bearing measurements taken and the number of simultaneously tracked ground objects is of interest. Obviously, increasing the number of tracked features should increase the navigation information content. Thus, our main thrust is focused on the quantification and measurement of the degree of observability of the optical bearings-only measurement arrangement. In this respect, we follow in the footsteps of [9] and [10]. The absolute minimal number of tracked features such that additional features do not further increase the degree of observability, is established.

Concerning observability: The measurement equations are time-dependent and therefore one cannot ascertain observability from an observability matrix. Hence, the information content of passive optical bearings-only measurements will be gauged by deriving the observability Grammian of the bearing-only measurement arrangement. It is however very important to first non-dimensionalize the navigation state, the bearings measurement geometry, and also the time variable, so that the derived observability Grammian is non-dimensional.This guarantees that the observability Grammian correctly reflects the geometry of the measurement arrangement, so that meaningful

conclusions can be drawn. The rank, or the condition number of the observability Grammian is established - it is the ultimate purveyor of the navigation potential of vision.

A word of caution concerning information fusion is in order. It is often much too easy to set up a Kalman Filter (KF) for fusing, e.g., optical and inertial measurements - in which case one then refers to INS aiding using bearings-only measurements [11]. The point is that a KF output will always be available. Even in the extreme case of an optical measurement arrangement where observability is non-existent, a KF can be constructed and a valid navigation state estimate output will be available, except that no aiding action is actually taking place: the produced navigation state estimate then exclusively hinges on prior information only - in this case, inertial measurements, whereas the optical measurements don't at all come into play.

In light of the above discussion, the real question is whether there is aiding action so that the optical measurements are actually brought to bear on a KF provided navigation state estimate, thus yielding enhanced estimation performance relative to a stand alone INS. One would like to determine how strong the aiding action is and into precisely which components of the navigation state the aiding action trickles down into. The answer is provided by our deterministic observability analysis:

A KF will help enhance the accuracy of the complete navigation state if, and only if, the system is observable, that is, the observability Grammian is full rank. We'll also address the case of partial observability.

Strictly speaking, the herein outlined analysis should be carried out whenever the use of a KF is contemplated, to get a better understanding of the data fusion process. For example, it is known that when during cruise, GPS position measure-

ments are used to aid an INS, no aiding action will be realized in the critical aircraft heading navigation state variable, unless the aircraft is performing high-g horizontal turns. And in the extreme case of an object in free fall - for example, a bomb - it can be shown that GPS position measurements will not enhance the estimate of any of the object's Euler angles.

Naturally, the use of bearings-only measurements can yield information on angular components only of an air vehicle's navigation state. We refer to the measurement of the aircraft "drift" angles, namely, the angles included between the ground referenced velocity vector and the aircraft body axes. A dramatic improvement in the navigation state information can be obtained if additional passive measurements become available. A case in point is baro-altitude measurement. The latter is also used in inertial navigation - to the extent that high precision inertial navigation is not possible without passive baro altitude, or, GPS - provided, altitude information. Indeed, the combined use of optical measurements and baro-altitude for navigation has a long history, from the days when navigators where seated in the glazed nose of aircraft and would optically track a ground feature using a driftmeter, or, on the continent, a cinemoderivometer.

We are also interested in the use of additional passive measurements and side information. We refer to known landmarks, digital terrain elevation data, LADAR provided range measurements, GPS provided position measurements, and, finally, the mechanization of an autonomous navigation system akin to an INS which however exclusively and continuously uses bearing measurements of ground features - one would then refer to an Optical Navigation System (ONS).

By augmenting the navigation state with the coordinates of the tracked ground features/objects, Simultaneous Location and Mapping (SLAM) is achieved in a unified

framework. Furthermore, the analysis can be extended to include the tracking of moving objects, whether on the ground, or in the air. Under standard kinematic assumptions, the motion of own ship relative to said tracked objects can be measured: think of obstacle avoidance or "see and avoid" guidance.

3.2.2 Modeling. We are cognizant of the fact that the degree of INS aiding provided by bearing measurements might strongly depend on the trajectory flown. For example, this certainly is the case when GPS position measurements are used for INS aiding. All this notwithstanding, in this study we confine our attention to the most basic two-dimensional scenario where the aircraft is flying wings level at constant altitude in the vertical plane. The two-dimensional scenario under consideration is illustrated in Figure3.1.

In 2-D, the navigation state is

$$X = (x, z, v_x, v_z, \theta)$$

and the "disturbance"

$$d = (\delta f_x, \delta f_z, \delta\omega)$$

consists of the biases δf_x and δf_z of the accelerometers and the bias $\delta\omega$ of the rate gyro. The error equations are

$$\delta\dot{X} = A\delta X + \Gamma d \tag{3.1}$$

We assume the Earth is flat and non-rotating - this, in view of the short duration and the low speed of the Micro Air Vehicle (MAV) under consideration. Consequently, in level flight the dynamics are

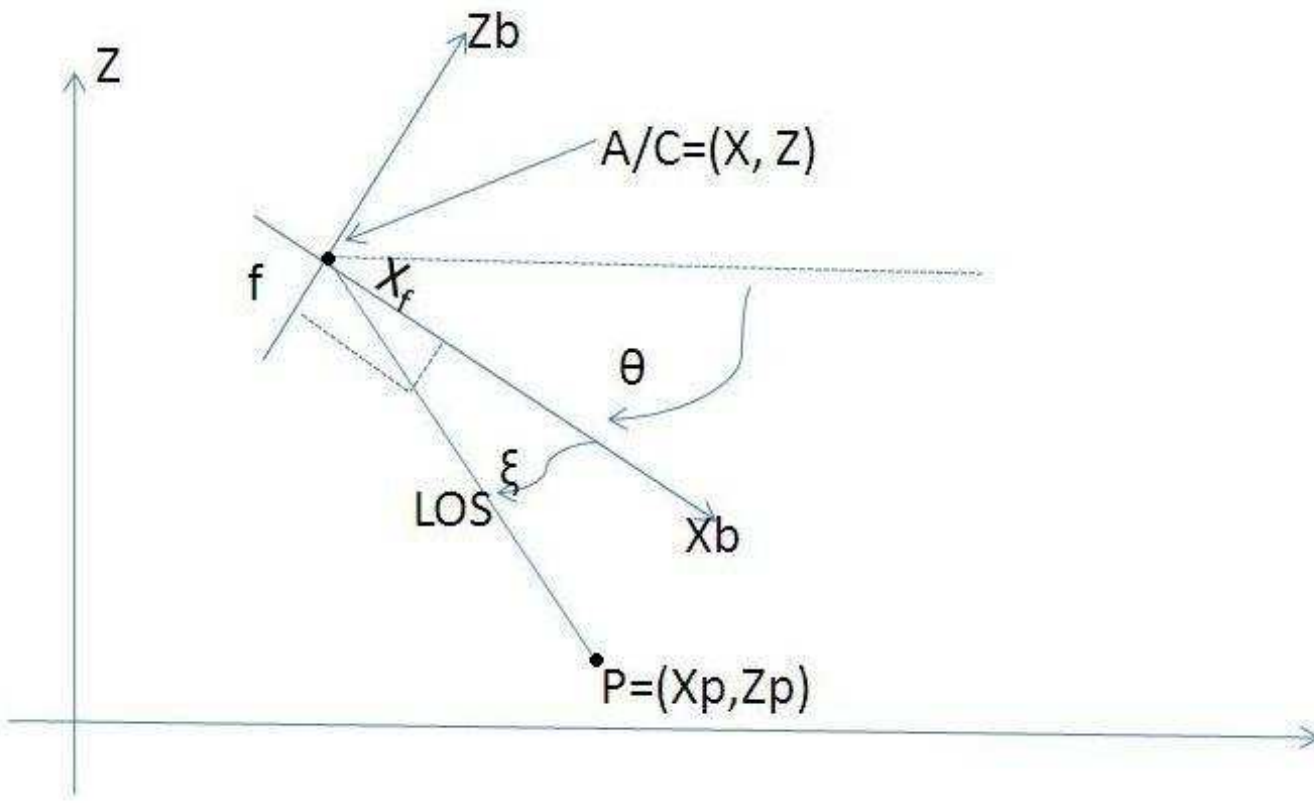

Figure 3.1: Flight in the vertical plane.

$$A = \begin{bmatrix} 0 & 0 & 1 & 0 & 0 \\ 0 & 0 & 0 & 1 & 0 \\ 0 & 0 & 0 & 0 & g \\ 0 & 0 & 0 & 0 & 0 \\ 0 & 0 & 0 & 0 & 0 \end{bmatrix}, \qquad \Gamma = \begin{bmatrix} 0 & 0 & 0 \\ 0 & 0 & 0 \\ 1 & 0 & 0 \\ 0 & 1 & 0 \\ 0 & 0 & 1 \end{bmatrix} \tag{3.2}$$

The tracked ground object is located at $P = (x_p, z_p)$. From the 2-D geometry in Fig3.1 we derive the measurement equation:

$$\frac{x_p - x}{z - z_p} = \cot(\theta + \xi) \tag{3.3}$$

and thus the measurement

$$\tan(\xi) = \frac{z - z_p - (x_p - x)\tan\theta}{x_p - x + (z - z_p)\tan\theta} = \frac{f}{x_f} \tag{3.4}$$

or

$$x_f = \frac{x_p - x + (z - z_p)\tan\theta}{z - z_p - (x_p - x)\tan\theta}\, f \tag{3.5}$$

Now, the INS output $x_c = x + \delta x$, $z_c = z + \delta z$, $\theta_c = \theta + \delta\theta$ where x, z and θ are the true navigation states. In order to linearize the measurement equation, we need the information x_p^-, z_p^-, that is, prior information on the position of the tracked ground feature.

Let

$$x_p^- = x_p + \delta x_p \tag{3.6}$$

$$z_p^- = z_p + \delta z_p \tag{3.7}$$

The true augmented state

$$x = x_c - \delta x \tag{3.8}$$

$$z = z_c - \delta z \tag{3.9}$$

$$v_x = v_{x_c} - \delta v_x \tag{3.10}$$

$$v_z = v_{z_c} - \delta v_z \tag{3.11}$$

$$\theta = \theta_c - \delta\theta \tag{3.12}$$

$$x_p = x_p^- - \delta x_p \tag{3.13}$$

$$z_p = z_p^- - \delta z_p \tag{3.14}$$

where $\delta x, \delta z, \delta v_x, \delta v_z, \delta\theta, \delta x_p, \delta z_p$ are the augmented state's estimation errors.

During level flight, and using the small angle approximation, the measurement equation is

$$\frac{x_f}{f} = \frac{x_p - x + (z - z_p)\theta}{z - z_p - (x_p - x)\theta} \tag{3.15}$$

and the measurement, expressed as a function of the state perturbations $\delta x, \delta z, \delta\theta, \delta x_p, \delta z_p$ is:

$$\frac{x_f}{f} = \frac{x_p^- - \delta x_p - x_c + \delta x + (z_c - \delta z - z_p^- + \delta z_p) \cdot (\theta_c - \delta\theta)}{z_c - \delta z - z_p^- + \delta z_p - (x_p^- - \delta x_p - x_c + \delta x) \cdot (\theta_c - \delta\theta)} \tag{3.16}$$

$$= \frac{x_p^- - x_c + (z_c - z_p^-)\theta_c + \delta x - \theta_c \delta z + (z_p^- - z_c)\delta\theta - \delta x_p + \theta_c \delta z_p}{z_c - z_p^- + (x_c - x_p^-)\theta_c - \theta_c \delta x - \delta z + (x_p^- - x_c)\delta\theta + \theta_c \delta x_p + \delta z_p}$$

$$= \frac{x_p^- - x_c + (z_c - z_p^-)\theta_c}{z_c - z_p^- + (x_c - x_p^-)\theta_c} + \frac{1}{\left[z_c - z_p^- + (x_c - x_p^-)\theta_c\right]^2} \cdot \{ \; [z_c - z_p^- + (x_c - x_p^-)\theta_c$$

$$+ (x_p^- - x_c + (z_c - z_p^-)\theta_c)\theta_c]\delta x$$

$$+ \left[-(z_c - z_p^- + (x_c - x_p^-)\theta_c)\theta_c + x_p^- - x_c + (z_c - z_p^-)\theta_c\right] \delta z$$

$$+ \left[(z_c - z_p^- + (x_c - x_p^-)\theta_c)(z_p^- - z_c) + (x_p^- - x_c + (z_c - z_p^-)\theta_c)(x_c - x_p^-)\right] \delta\theta$$

$$+ \left[z_p^- - z_c + (x_p^- - x_c)\theta_c + (x_c - x_p^- + (z_p^- - z_c)\theta_c)\theta_c\right] \delta x_p$$

$$+ \left[(z_c - z_p^- + (x_c - x_p^-)\theta_c)\theta_c + x_c - x_p^- + (z_p^- - z_c)\theta_c\right] \delta z_p \; \}$$

$$= \frac{x_p^- - x_c + (z_c - z_p^-)\theta_c}{z_c - z_p^- + (x_c - x_p^-)\theta_c} + \frac{1}{\left[z_c - z_p^- + (x_c - x_p^-)\theta_c\right]^2} \cdot \{ \; \left[z_c - z_p^- + (z_c - z_p^-)\theta_c^2\right] \delta x$$

$$+ \left[x_p^- - x_c + (x_p^- - x_c)\theta_c^2\right] \delta z - \left[(x_p^- - x_c)^2 + (z_p^- - z_c)^2\right] \delta\theta + \left[z_p^- - z_c + (z_p^- - z_c)\theta_c^2\right] \delta x_p$$

$$+\left[x_c - x_p^- + (x_c - x_p^-)\theta_c^2\right]\delta z_p\ \}$$

$$= \frac{x_p^- - x_c + (z_c - z_p^-)\theta_c}{z_c - z_p^- + (x_c - x_p^-)\theta_c} + \frac{1}{\left[z_c - z_p^- + (x_c - x_p^-)\theta_c\right]^2} \cdot \left[(1+\theta_c^2)(z_c - z_p^-)\delta x + (1+\theta_c^2)(x_p^- - x_c)\delta z\right.$$

$$\left. - \left[(x_p^- - x_c)^2 + (z_p^- - z_c)^2\right]\delta\theta + (1+\theta_c^2)(z_p^- - z_c)\delta x_p + (1+\theta_c^2)(x_c - x_p^-)\delta z_p\ \right]$$

$$= \frac{x_p^- - x_c + (z_c - z_p^-)\theta_c}{z_c - z_p^- + (x_c - x_p^-)\theta_c} + \frac{1+\theta_c^2}{\left[z_c - z_p^- + (x_c - x_p^-)\theta_c\right]^2} \cdot \{\ (z_c - z_p^-)\delta x + (x_p^- - x_c)\delta z$$

$$-[(x_p^- - x_c)^2 + (z_p^- - z_c)^2]\delta\theta + (z_p^- - z_c)\delta x_p + (x_c - x_p^-)\delta z_p\ \}$$

We use the fact that the navigation state errors are small and therefore the formula $\frac{1}{1+x} \approx 1 + x$ is repeatedly used in derivations above to simplify the measurement equation and to linearize it.

Hence, for level flight the linearized measurement equation is

$$\frac{x_f}{f} - \frac{x_p^- - x_c + (z_c - z_p^-)\theta_c}{z_c - z_p^- + (x_c - x_p^-)\theta_c} = \frac{1}{\left[z_c - z_p^- + (x_c - x_p^-)\theta_c\right]^2} \cdot \{\ (z_c - z_p^-)\delta x$$

$$+(x_p^- - x_c)\delta z - [(x_p^- - x_c)^2 + (z_p^- - z_c)^2]\delta\theta + (z_p^- - z_c)\delta x_p + (x_c - x_p^-)\delta z_p\ \} \qquad (5)$$

3.2.3 Special Cases. If the position $(x_p,\ z_p)$ of the tracked ground object is *known*, the state is the navigation state x, z, v_x, v_z, θ and the linearized measurement equation is

$$\frac{x_f}{f} - \frac{x_p - x_c + (z_c - z_p)\theta_c}{z_c - z_p + (x_c - x_p)\theta_c} = \frac{1}{[z_c - z_p + (x_c - x_p)\theta_c]^2} \cdot \{ (z_c - z_p)\delta x + (x_p - x_c)\delta z$$

$$+[(x_p - x_c)^2 + (z_p - z_c)^2]\delta\theta \}$$

If only the *elevation* z_p of the tracked ground object is known, the augmented state is $x, z, v_x, v_z, \theta, x_p$. Without loss of generality we set $z_p = 0$, and the linearized measurement equation is:

$$\frac{x_f}{f} - \frac{x_p^- - x_c + z_c\theta_c}{z_c + (x_c - x_p^-)\theta_c} = \frac{1}{[z_c + (x_c - x_p^-)\theta_c]^2} \cdot \{ z_c\delta x + (x_p^- - x_c)\delta z$$

$$+[(x_p^- - x_c)^2 + z_c^2]\delta\theta - z_c\delta x_p \}$$

Remark : For the purpose of analysis, on the right hand side of the measurement equation one can replace x_c by the true - that is, the nominal - state component x , z_c by the true - that is, the nominal - state component z, and θ_c by $\theta \equiv 0$.

Hence, if the position of the tracked ground object is known, and, in addition, without loss of generality we set $z_p = 0$, then the linearized measurement equation is

$$\frac{x_f}{f} - \frac{x_p - x_c + z_c\theta_c}{z_c + (x_c - x_p)\theta_c} = \frac{1}{z^2} \cdot \left\{ z\delta x + (x_p - x)\delta z - [(x_p - x)^2 + z^2]\delta\theta \right\} \qquad (3.17)$$

If only the elevation z_p of the tracked ground object is known, and, as before without loss of generality, we set $z_p = 0$, then the state error is $\delta x, \delta z, \delta v_x, \delta v_z, \delta\theta, \delta x_p$, and the linearized measurement equation is

$$\frac{x_f}{f} - \frac{x_p^- - x_c + z\theta_c}{z_c + (x - x_p)\theta_c} = \frac{1}{z^2} \cdot \left\{ z\delta x + (x_p^- - x)\delta z - [(x_p^- - x)^2 + z^2]\delta\theta - z\delta x_p \right\} \quad (3.18)$$

If the position of the ground object is not known, the navigation state error is $\delta x, \delta z, \delta v_x, \delta v_z, \delta\theta, \delta x_p, \delta z_p$ and the linearized measurement equation - see, e.g., eq.(5) - is

$$\frac{x_f}{f} - \frac{x_p^- - x_c + (z - z_p^-)\theta_c}{z - z_p^- + (x - x_p^-)\theta_c} = \frac{1}{(z - z_p^-)^2} \cdot \{ (z - z_p^-)\delta x + (x_p^- - x)\delta z$$

$$-[(x_p^- - x)^2 + (z - z_p^-)^2]\delta\theta + (z - z_p^-)\delta x_p + (x - x_p^-)\delta z_p \}$$

Furthermore, for the purpose of analysis, on the right hand side of the last two equations we can also replace x_p^- and z_p^- by the true position (x_p, z_p) of the tracked object. Hence the respective measurement equations are

$$\frac{x_f}{f} - \frac{x_p^- - x_c + z\theta_c}{z_c + (x - x_p)\theta_c} = \frac{1}{z^2} \cdot \left\{ z\delta x + (x_p - x)\delta z - [(x_p - x)^2 + z^2]\delta\theta - z\delta x_p \right\} \quad (3.19)$$

and

$$\frac{x_f}{f} - \frac{x_p^- - x_c + (z - z_p^-)\theta_c}{z - z_p^- + (x - x_p^-)\theta_c} = \frac{1}{(z - z_p)^2} \cdot \{ (z - z_p)\delta x + (x_p - x)\delta z$$

$$-[(x_p - x)^2 + (z - z_p)^2]\delta\theta + (z - z_p)\delta x_p + (x - x_p)\delta z_p \}$$

Furthermore, without loss of generality, in the last equation we set $z_p = 0$:

$$\frac{x_f}{f} - \frac{x_p^- - x_c + (z - z_p^-)\theta_c}{z - z_p^- + (x - x_p^-)\theta_c} = \frac{1}{z^2} \cdot \{ z\delta x + (x_p - x)\delta z$$

$$-[(x_p - x)^2 + z^2]\delta\theta + z\delta x_p + (x - x_p)\delta z_p \}$$

During the initial geo-location phase where one is exclusively interested in the ground object's position, one takes the INS calculated aircraft navigation state variables x, z, θ at face value and the linearized measurement equation is used to estimate $\delta x_p, \delta z_p$:

$$\frac{x_f}{f} - \frac{x_p^- - x + (z - z_p^-)\theta}{z - z_p^- + (x - x_p^-)\theta} = \frac{1}{(z - z_p^-)^2} \cdot \left[(z_p^- - z)\delta x_p + (x - x_p^-)\delta z_p\right] \tag{3.20}$$

This equation would be used if a recursive geo - location algorithm is applied. Note however that if one is exclusively interested in geo - locating the ground object, a batch algorithm might be preferable. Finally, one would use Equation (3.19) and iterate

$$x_p^- := x_p^- - \delta x_p \tag{3.21}$$

$$z_p^- := z_p^- - \delta z_p \tag{3.22}$$

In practice, the first guesses of x_p^- and z_p^- are generated as follows. We have the INS provided "prior" information on the navigation state x, z, θ. Bearing measurements of the ground feature P are taken over time. One can use the first two bearing measurements to obtain the "prior" x_p^- and z_p^- information. Hence, initially one is exclusively concerned with the geo - location of the feature on the ground. To this end one uses Equation (3.3) and upon recording two measurements one obtains a set of two linear equations in the unknowns x_p^- and z_p^- :

$$x_p + \cot(\theta_{c_1} + \xi_{m_1})z_p = x_{c_1} + z_{c_1}\cot(\theta_{c_1} + \xi_{m_1}) \tag{3.23}$$

$$x_p + \cot(\theta_{c_2} + \xi_{m_2}) z_p = x_{c_2} + z_{c_2} \cot(\theta_{c_2} + \xi_{m_2}) \tag{3.24}$$

whereupon

$$\begin{pmatrix} x_p^- \\ z_p^- \end{pmatrix} = \frac{1}{\cot(\theta_{c_2}+\xi_{m_2}) - \cot(\theta_{c_1}+\xi_{m_1})} \cdot \begin{bmatrix} \cot(\theta_{c_2} + \xi_{m_2}) & -\cot(\theta_{c_1} + \xi_{m_1}) \\ -1 & 1 \end{bmatrix}$$

$$\cdot \begin{pmatrix} x_{c_1} + z_{c_1} \cot(\theta_{c_1} + \xi_{m_1}) \\ x_{c_2} + z_{c_2} \cot(\theta_{c_2} + \xi_{m_2}) \end{pmatrix}$$

Obviously, one could use more than two bearing measurements and obtain an overdetermined linear system in x_p^- and z_p^-, but then one performs geo-location only and completely forgoes the task of INS aiding. Since at time instants $k = 1$ and $k = 2$ the INS is not aided, the original prior information on the navigation state eror δx^-, δz^-, $\delta\theta^-$ must be propagated forward to time step $k = 2$. From this point on, the updated prior information δx^-, δz^-, $\delta\theta^-$ and the prior information x_p^- and z_p^- are employed to start the Kalman filter such that the aircraft navigation state and the ground object's position are simultaneously updated using the bearing measurements obtained at time $k = 3, 4....$ In conclusion: When unknown ground objects are tracked, they first must be geo - located. This delays the INS aiding action by at least two time steps. Furthermore, the aircraft's navigation state prior information must be propagated ahead two time steps, without it being updated with bearing measurements, while one exclusively relies on the INS. The measurement equation is then re- linearized using the ground object's prior information obtained during the preliminary geo - location step, and the two time steps propagated ahead navigation state prior information. From this point on, the INS aiding action and the ground object's geo - location is simultaneously performed during the ground object's tracking interval.

If the ground object's elevation z_p is known, say from a digital terrain data-base, one can make do with one bearing measurement only:

$$x_p^- = x_c + (z_c - z_p)\cot(\theta_c + \xi_m) \tag{3.25}$$

3.2.4 Nondimentional Variables. The aircraft's nominal altitude is h and its nominal ground speed is v. Set

$$x \to \tfrac{x}{h}, z \to \tfrac{z}{h}, v_x \to \tfrac{v_x}{v}, v_z \to \tfrac{v_z}{v}, t \to \tfrac{tv}{h}, T \to \tfrac{v}{h}T, \delta f_x \to \tfrac{\delta f_x}{g}, \delta f_z \to \tfrac{\delta f_z}{g}, \ \delta\omega \to \tfrac{h}{v}\delta\omega.$$

Introduce the non-dimentional parameter ($\frac{1}{2}$ the ratio of the aircraft's potential energy to its kinetic energy):

$$a \equiv \frac{hg}{v^2}$$

Then the aircraft's non-dimentional navigation state error dynamics are specified by the matrices

$$A = \begin{bmatrix} 0 & 0 & 1 & 0 & 0 \\ 0 & 0 & 0 & 1 & 0 \\ 0 & 0 & 0 & 0 & a \\ 0 & 0 & 0 & 0 & 0 \\ 0 & 0 & 0 & 0 & 0 \end{bmatrix}, \Gamma = \begin{bmatrix} 0 & 0 & 0 \\ 0 & 0 & 0 \\ a & 0 & 0 \\ 0 & a & 0 \\ 0 & 0 & 1 \end{bmatrix} \tag{3.26}$$

The scenario considered is wings level flight in the vertical plane (x, z).

For example, for a MAV, $v = 20$ $[\frac{m}{sec}]$, $h = 40$ [m], and $g = 10$ $[\frac{m}{sec^2}]$ $\Rightarrow$ $a = 1$.

The geometry of the measurement scenario is characterized by the two non-dimensional parameters

$$\alpha_1 = \tan \eta_1$$

$$\alpha_2 = \tan \eta_2$$

Consequently, the non-dimensional measurement interval

$$T = \tan \eta_1 + \tan \eta_2 \tag{3.27}$$

Consider first a symmetric measurement scenario where $\eta_1 = \eta_2 = \eta$. Since $x = vt$, $x_p = h \tan \eta$, using nondimensional variables, we obtain from the measurement Equation (3.17)

$$y = \delta x + (\tan \eta - t)\delta z - [1 + (\tan \eta - t)^2]\delta\theta, \tag{3.28}$$

$$0 \leq t \leq 2 \tan \eta$$

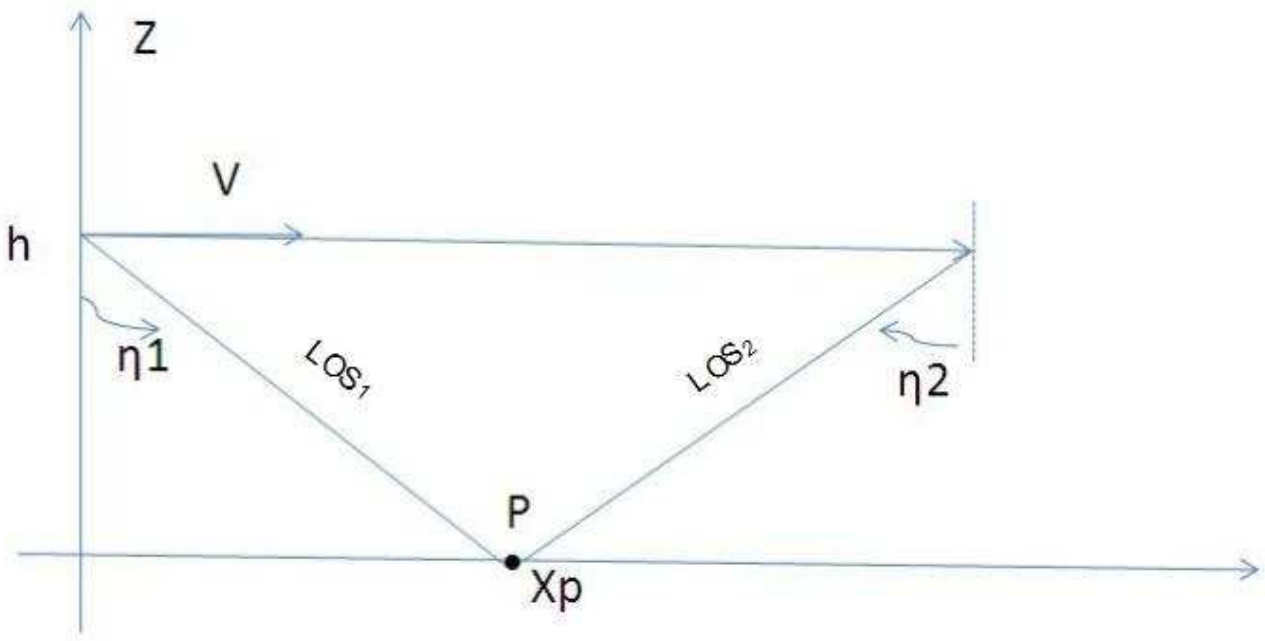

Figure 3.2: Simple Measurement Scenario

i.e., the measurement matrix

$$C = \left[1, \quad \tan\eta - t, \quad 0, \quad 0, \quad 2t\tan\eta - t^2 - \tfrac{1}{\cos^2\eta}\right] \ , \tag{3.29}$$

the measurement

$$y \equiv \frac{x_f}{f} - \frac{x_p - x_c + z_c\theta_c}{z_c + (x_c - x_p)\theta_c} \tag{3.30}$$

and the measurement interval

$$T = \tfrac{h}{v}(\tan\eta_1 + \tan\eta_2)$$

Note that, as is often the case in INS aiding, the measurement matrix C is time dependent.

3.2.5 Observability. The observability Grammian [12] is

$$W(T) = \int_0^T e^{A^T t} C^T(t) C(t) e^{At} dt \tag{3.31}$$

where T is the measurement interval.

We calculate

$$e^{At} = \begin{bmatrix} 1 & 0 & t & 0 & \frac{1}{2}at^2 \\ 0 & 1 & 0 & t & 0 \\ 0 & 0 & 1 & 0 & at \\ 0 & 0 & 0 & 1 & 0 \\ 0 & 0 & 0 & 0 & 1 \end{bmatrix} \tag{3.32}$$

The geometry of the symmetric measurement arrangement is specified by the non-dimensional parameter $\alpha \equiv \tan\eta$. Then the non-dimentional observation interval $T = 2\alpha$ and the measurement matrix

$$C(t) = \begin{bmatrix} 1, & \alpha - t, & 0, & 0, & -1 - (\alpha - t)^2 \end{bmatrix} \tag{3.33}$$

We calculate

$$C(t)e^{At} = \begin{bmatrix} 1, & \alpha - t, & t, & (\alpha - t)t, & \frac{1}{2}at^2 - 1 - (\alpha - t)^2 \end{bmatrix} \tag{3.34}$$

and

$$e^{A^T t}C^T(t)C(t)e^{At} = \begin{bmatrix} 1 & \alpha - t & t & (\alpha - t)t & f(t) \\ \alpha - t & (\alpha - t)^2 & (\alpha - t)t & (\alpha - t)^2 t & (\alpha - t)f(t) \\ t & (\alpha - t)t & t^2 & (\alpha - t)t^2 & tf(t) \\ (\alpha - t)t & (\alpha - t)^2 t & (\alpha - t)t^2 & (\alpha - t)^2 t^2 & (\alpha - t)tf(t) \\ f(t) & (\alpha - t)f(t) & tf(t) & t(\alpha - t)f(t) & f^2(t) \end{bmatrix} \tag{3.35}$$

where $f(t) \equiv \frac{1}{2}at^2 - 1 - (a - t)^2$. We integrate the time-dependent entries of the matrix in Equation (3.35) and obtain the observability Grammian elements.

$$W_{1,1} = 2\alpha, W_{1,2} = 0, W_{1,3} = 2\alpha^2, W_{1,4} = -\frac{2}{3}\alpha^3, W_{1,5} = \frac{4}{3}a\alpha^3 - 2\alpha - \frac{2}{3}\alpha^3, \tag{3.36}$$

$$W_{2,2} = \frac{2}{3}\alpha^3, W_{2,3} = -\frac{2}{3}\alpha^3, W_{2,4} = \frac{2}{3}\alpha^4, W_{2,5} = 2\alpha^2 - 2\alpha^3 - \frac{2}{3}a\alpha^4, \tag{3.37}$$

$$W_{3,3} = \frac{8}{3}\alpha^4, W_{3,4} = -\frac{4}{3}\alpha^4, W_{3,5} = 2a\alpha^4 - \frac{2}{3}\alpha^4 - 2\alpha^2, \tag{3.38}$$

$$W_{4,4} = \frac{16}{15}\alpha^5, W_{4,5} = \frac{2}{5}\alpha^5 - \frac{6}{5}a\alpha^5 + \frac{2}{3}\alpha^4, \tag{3.39}$$

$$W_{5,5} = (\frac{2}{5} - \frac{16}{15}a + \frac{8}{5}a^2)\alpha^5 + \frac{4}{3}(1-2a)\alpha^3 + 2\alpha \tag{3.40}$$

Consider the MAV scenario where $a = 1$ and the measurement scenario shown in the Figure 3.2, where $\alpha = 1$

The observability Grammian is then

$$W = \frac{2}{15}\begin{bmatrix} 15 & 0 & 15 & -5 & -10 \\ 0 & 5 & -5 & 5 & -5 \\ 15 & -5 & 20 & -10 & -5 \\ -5 & 5 & -10 & 8 & -1 \\ -10 & -5 & -5 & -1 & 12 \end{bmatrix} \tag{3.41}$$

The 5×5 real, symmetric, positive, semi-definite matrix W is not full rank: Rank $(W) = 3$. This implies:no observability.

Next, consider the alternative measurement geometry where the tracked ground feature P is at the origin ($x_p = 0$). Then $\eta = 0$ so that $\alpha = 0$ and

$$e^{A^T t}C^T(t)C(t)e^{At} = \begin{bmatrix} 1 & -t & t & -t^2 & f(t) \\ -t & t^2 & -t^2 & t^3 & -f(t)\cdot t \\ t & -t^2 & t^2 & -t^3 & f(t)\cdot t \\ -t^2 & t^3 & -t^3 & t^4 & -f(t)\cdot t^2 \\ f(t) & -f(t)\cdot t & f(t)\cdot t & -f(t)\cdot t^2 & 2f^2(t) \end{bmatrix}$$

where $f(t) = \frac{1}{2}(a-1)t^2 - 1$

The non-dimensional measurement interval $T = 2$, and the elements of the observability Grammian are

$W_{1,1} = 2$, $W_{1,2} = -2$, $W_{1,3} = 2$, $W_{1,4} = -\frac{8}{3}$, $W_{1,5} = \frac{2}{3}(2a-7)$,
$W_{2,2} = \frac{8}{3}$, $W_{2,3} = -\frac{8}{3}$, $W_{2,4} = 4$, $W_{2,5} = 2(3-a)$,
$W_{3,3} = \frac{8}{3}$, $W_{3,4} = -4$, $W_{3,5} = 2(a-3)$,
$W_{4,4} = \frac{32}{5}$, $W_{4,5} = \frac{8}{15}(17-6a)$,
$W_{5,5} = \frac{32}{5}(\frac{1}{2}a-1)^2 + \frac{8}{3}(2-a) + 2$

As before, assume $a = 1$. The observability Grammian is

$$W = \frac{2}{15}\begin{bmatrix} 15 & -15 & 15 & -20 & -25 \\ -15 & 20 & -20 & 30 & 30 \\ 15 & -20 & 20 & -30 & -30 \\ -20 & 30 & -30 & 48 & 44 \\ -25 & 30 & -30 & 44 & 47 \end{bmatrix} \tag{3.42}$$

The matrix W has two identical columns (columns 2 and 3) and two identical rows, rows 2 and 3. This implies Rank $(W) = 3$.

When both features are tracked, the observation matrix is the 2×5 matrix.

$$C(t) = \begin{bmatrix} 1 & 1-t & 0 & 0 & 2t-t^2-2 \\ 1 & -t & 0 & 0 & -1-t^2 \end{bmatrix} \tag{3.43}$$

As before, for $a = 1$ we obtain

$$e^{At} = \begin{bmatrix} 1 & 0 & t & 0 & \frac{1}{2}t^2 \\ 0 & 1 & 0 & t & 0 \\ 0 & 0 & 1 & 0 & t \\ 0 & 0 & 0 & 1 & 0 \\ 0 & 0 & 0 & 0 & 1 \end{bmatrix} \tag{3.44}$$

and we calculate

$$C(t)e^{At} = \begin{bmatrix} 1 & 1-t & t & t-t^2 & 2t-\frac{1}{2}t^2-2 \\ 1 & -t & t & -t^2 & -\frac{1}{2}t^2-1 \end{bmatrix} \tag{3.45}$$

and $e^{A^T t}C^T(t)C(t)e^{At} =$

$$\begin{bmatrix} 2 & 1-2t & 2t & t-2t^2 & 2t-t^3-3 \\ 1-2t & 1+2t^2-2t & t-2t^2 & t-2t^2+2t^3 & t^3-\frac{5}{2}t^2+5t-2 \\ 2t & t-2t^2 & 2t^2 & t^2-2t^3 & 2t^2-t^3-3t \\ t-2t^2 & t-2t^2+2t^3 & t^2-2t^3 & 2t^4-2t^3+t^2 & t^4-\frac{5}{2}t^3+5t^2-2t \\ 2t-t^2-3 & t^3-\frac{5}{2}t^2+5t-2 & 2t^2-t^3-3t & t^4-\frac{5}{2}t^3+5t^2-2t & \frac{1}{2}t^4-2t^3+7t^2-8t+5 \end{bmatrix}$$

Integration yields the entries of the observability Grammian

$W_{1,1} = 30$, $W_{1,2} = -15$, $W_{1,3} = 30$, $W_{1,4} = -25$, $W_{1,5} = -35$,
$W_{2,2} = 25$, $W_{2,3} = -25$, $W_{2,4} = 35$, $W_{2,5} = 25$,
$W_{3,3} = 40$, $W_{3,4} = -40$, $W_{3,5} = -35$,
$W_{4,4} = 56$, $W_{4,5} = 43$,
$W_{5,5} = 59$

The matrix W is full rank. Hence, we have observability.

Concerning a shortcut: A sufficient condition for observability is $rank(W) = 5$, where $W = W_{p_1} + W_{p_2}$ and W_{p_i} is the observability Grammian when ground object i is tracked, $i = 1, 2$; this is indeed the case.

3.2.6 Only the Elevation z_p of the Tracked Ground Object is Known. The augmented state's error is $(\delta x, \delta z, \delta v_x, \delta v_z, \delta\theta, \delta x_p)^T \in \Re^6$. Set $x_p \rightarrow \frac{x_p}{h}$.

The augmented system's dynamics are specified by

$$A_a := \begin{bmatrix} A & \vdots & 0 \\ \cdots & \vdots & \cdots \\ 0 & \vdots & 0 \end{bmatrix}_{6\times 6}, \Gamma_a := \begin{bmatrix} \Gamma \\ \cdots \\ 0 \end{bmatrix}_{6\times 3} \tag{3.46}$$

$$C_a(t) := (C(t), -1) \tag{3.47}$$

where, recall, for wings level, constant altitude flight,

$$A = \begin{bmatrix} 0 & 0 & 1 & 0 & 0 \\ 0 & 0 & 0 & 1 & 0 \\ 0 & 0 & 0 & 0 & a \\ 0 & 0 & 0 & 0 & 0 \\ 0 & 0 & 0 & 0 & 0 \end{bmatrix}, \Gamma = \begin{bmatrix} 0 & 0 & 0 \\ 0 & 0 & 0 \\ a & 0 & 0 \\ 0 & a & 0 \\ 0 & 0 & 1 \end{bmatrix} \tag{3.48}$$

and

$$C(t) = \begin{bmatrix} 1, & \alpha - t, & 0, & 0, & 2\alpha t - t^2 - 1 - \alpha^2 \end{bmatrix} \tag{3.49}$$

We calculate

$$e^{A_a t} := \begin{bmatrix} e^{At} & \vdots & 0 \\ \cdots & \vdots & \cdots \\ 0 & \vdots & 1 \end{bmatrix} \tag{3.50}$$

$$C_a e^{A_a t} = (Ce^{At}, -1) \tag{3.51}$$

$$e^{A^T t} C_a^T(t) C_a(t) e^{A_a t} = \begin{bmatrix} e^{A^T t} C^T C e^{At} & -e^{A^T} C^T \\ -Ce^{At} & 1 \end{bmatrix} \tag{3.52}$$

and

$$C(t)e^{At} = (1, \alpha - t, t, \alpha t - t^2, \frac{1}{2}at^2 - 1 - \alpha^2 - t^2 + 2\alpha t) \tag{3.53}$$

Let

$$w^T \equiv \int_0^{2\alpha} C(t)e^{At}dt = (2\alpha, 0, 2\alpha^2, -\frac{2}{3}\alpha^3, \frac{2}{3}(2a-1)\alpha^3 - 2\alpha) \tag{3.54}$$

$$W_a = \begin{pmatrix} W & -w \\ -w^T & 2\alpha \end{pmatrix} \tag{3.55}$$

When a = 1,

$$w^T = (2\alpha, 0, 2\alpha^2, -\frac{2}{3}\alpha^3, \frac{2}{3}\alpha^3 - 2\alpha) \tag{3.56}$$

and for $\alpha = 1$,

$$w^T = (2, 0, 2, -\frac{2}{3}, -\frac{4}{3}) \tag{3.57}$$

When $\alpha = 0$,

$$w^T = (2, -2, 2, -\frac{8}{3}, -\frac{10}{3}) \tag{3.58}$$

Hence, when $a = 1$ and $\alpha = 1$,

$$W_1 = \frac{2}{15}\begin{bmatrix} 15 & 0 & 15 & -5 & -10 & -15 \\ 0 & 5 & -5 & 5 & -5 & 0 \\ 15 & -5 & 20 & -10 & -5 & -15 \\ -5 & 5 & -10 & 8 & -1 & 5 \\ -10 & -5 & -5 & -1 & 12 & 10 \\ -15 & 0 & -15 & 5 & 10 & 30 \end{bmatrix} \tag{3.59}$$

When $a = 1$ and $\alpha = 0$

$$W_2 = \frac{2}{15}\begin{bmatrix} 15 & -15 & 15 & -20 & -25 & -15 \\ -15 & 20 & -20 & 30 & 30 & 15 \\ 15 & -20 & 20 & -30 & -30 & -15 \\ -20 & 30 & -30 & 48 & 44 & 20 \\ -25 & 30 & -30 & 44 & 47 & 25 \\ -15 & 15 & -15 & 20 & 25 & 15 \end{bmatrix} \tag{3.60}$$

Rank$(W_1) = 4$. and Rank $(W_2) = 3$. Rank $(W_1 + W_2) = 6$.

3.2.7 Partial Observability. When the observability Grammian W is rank deficient, that is,

$$rank(W) = r < n \ ,$$

where n is the state space dimension, the system is not observable; we then refer to the system as being partially observable. Strictly speaking, the aiding action of bearing-only measurements does not percolate into all the state components. One is thus interested in determining which states are (positively) impacted by the aiding action. The answer is provided by the Singular Value Decomposition (SVD) of the observability Garammian matrix W. The following holds:

The $n \times n$ real symmetric positive semi-definite matrix W can be factored as

$$W = HK$$

where H is a $n \times r$ matrix and K is a $r \times n$ matrix. Furthermore, $rank(H) = r$ and $rank(K) = r$; in other words, this is a full rank factorization.

From the SVD we conclude that the measurement process allows us to estimate the parameter $\theta \in \Re^r$:

$$\theta = (H^T H)^{-1} H^T \int_0^T e^{A^T t} C^T(t) y(t) dt$$

The latter is related to the navigation state X as follows.

$$\theta = K X_0 \tag{3.61}$$

The navigation information provided by the bearing measurements is encapsulated in Equation (3.61). The complete *initial* state X_0 cannot be calculated from the measurement record $y(t)$, $0 \leq t \leq T$ and in order to obtain a data driven estimate of the full state vector, $n - r$ additional independent measurements of the navigation state are needed. In 2-D, and when the position of the ground object is known, the dimension of the state, $n = 5$. When one known ground feature is tracked, $r = 3$. This tells us that two additional independent measurements of the navigation state are needed. The availability of the passively measured baro altitude immediately comes to mind, so that one additional independent measurement is needed for establishing the navigation state. The latter could be the aircraft's pitch angle θ, which is independently provided by a vertical gyroscope.

3.3 Flying in 3-D

Scenario: Nominal aircraft trajectory is wings level, constant altitude flight.

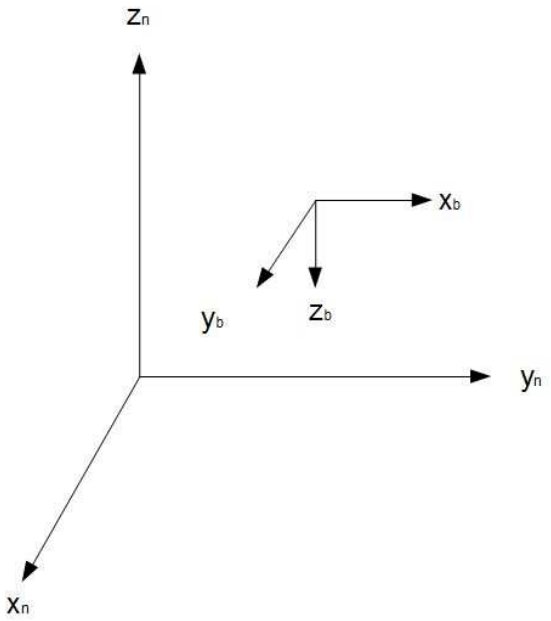

Figure 3.3: The Navigation and Body frames in 3 - D.

The information on the attitude errors is encapsulated in the vector $\delta\Psi$. The latter is not listing of the aircraft Euler angles errors. We first derive an expression for $\delta\Psi$ as a function of the Euler angles' errors.

In this section the relationship between the "attitude error" vector $\delta\Psi$ and the Euler angles errors $\delta\theta$, $\delta\psi$, $\delta\phi$ is established.
First, note that the nominal navigation to body axes DCM is

$$C_b^n = \begin{bmatrix} 0 & 1 & 0 \\ 1 & 0 & 0 \\ 0 & 0 & -1 \end{bmatrix} \tag{3.62}$$

Next, consider three relationships:

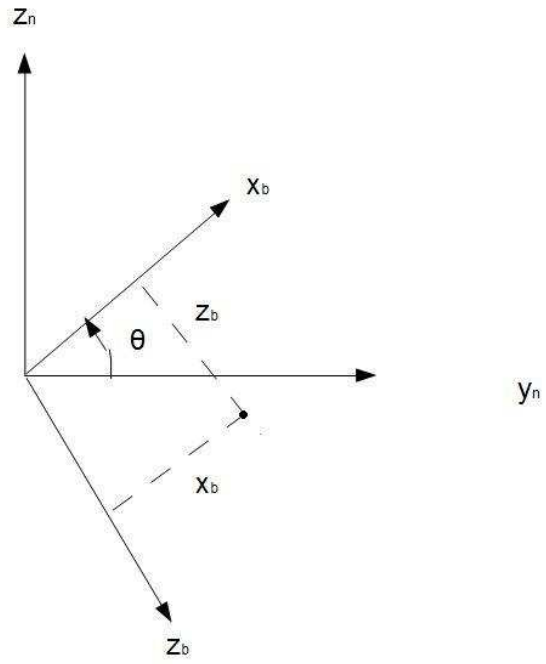

Figure 3.4: θ - Rotation.

3.3.1 θ - rotation. Since

$$y_n = x_b \cos\theta + z_b \sin\theta$$

$$z_n = x_b \sin\theta - z_b \cos\theta$$

$$x_n = y_b$$

$\Rightarrow$

$$\begin{pmatrix} x_n \\ y_n \\ z_n \end{pmatrix} = \begin{bmatrix} 0 & 1 & 0 \\ \cos\theta & 0 & \sin\theta \\ \sin\theta & 0 & -\cos\theta \end{bmatrix} \begin{pmatrix} x_b \\ y_b \\ z_b \end{pmatrix}$$

$\Rightarrow$

$$C_b^n(\theta) = \begin{bmatrix} 0 & 1 & 0 \\ \cos\theta & 0 & \sin\theta \\ \sin\theta & 0 & -\cos\theta \end{bmatrix}^2$$

and for small angles $\delta\theta$,

$$C_b^n = \begin{bmatrix} 0 & 1 & 0 \\ 1 & 0 & \delta\theta \\ \delta\theta & 0 & -1 \end{bmatrix}$$

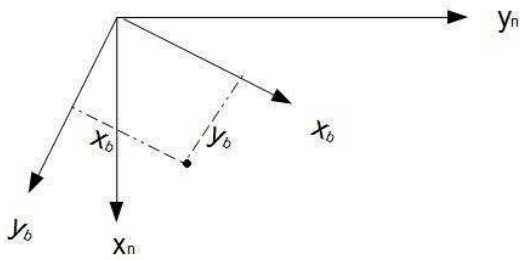

Figure 3.5: ψ - rotation.

3.3.2 ψ - rotation. Since

$$y_n = x_b \cos\psi - y_b \sin\psi$$

$$x_n = x_b \sin\psi + y_b \cos\psi$$

$$z_n = -z_b$$

$\Rightarrow$

$$\begin{pmatrix} x_n \\ y_n \\ z_n \end{pmatrix} = \begin{bmatrix} \sin\psi & \cos\psi & 0 \\ \cos\psi & -\sin\psi & 0 \\ 0 & 0 & -1 \end{bmatrix} \begin{pmatrix} x_b \\ y_b \\ z_b \end{pmatrix}$$

$\Rightarrow$

$$C_b^n(\psi) = \begin{bmatrix} \sin\psi & \cos\psi & 0 \\ \cos\psi & -\sin\psi & 0 \\ 0 & 0 & -1 \end{bmatrix}^2$$

and for small angles $\delta\psi$,

$$C_b^n = \begin{bmatrix} \delta\psi & 1 & 0 \\ 1 & -\delta\psi & 0 \\ 0 & 0 & -1 \end{bmatrix}$$

3.3.3 ϕ - rotation. Since

$$x_n = x_b \cos\phi - z_b \sin\phi$$

$$z_n = -z_b \cos\phi - y_b \sin\phi$$

$$y_n = x_b$$

$\Rightarrow$

$$\begin{pmatrix} x_n \\ y_n \\ z_n \end{pmatrix} = \begin{bmatrix} 0 & \cos\phi & -\sin\phi \\ 1 & 0 & 0 \\ 0 & -\sin\phi & -\cos\phi \end{bmatrix} \begin{pmatrix} x_b \\ y_b \\ z_b \end{pmatrix}$$

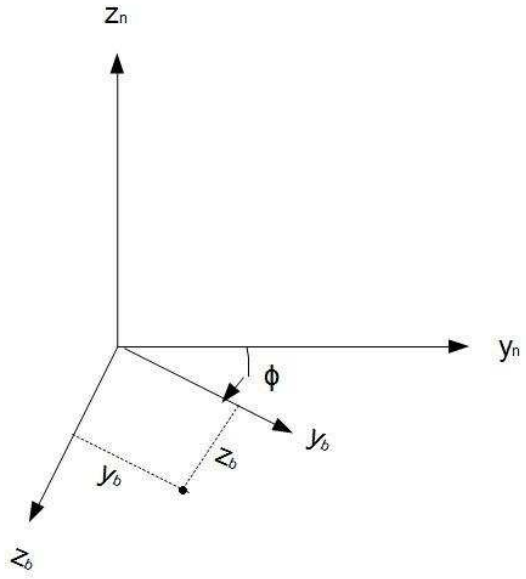

Figure 3.6: ψ - rotation.

$\Rightarrow$

$$C_b^n(\phi) = \begin{bmatrix} 0 & \cos\phi & -\sin\phi \\ 1 & 0 & 0 \\ 0 & -\sin\phi & -\cos\phi \end{bmatrix}$$

and for small angles $\delta\phi$,

$$C_b^n(\phi) = \begin{bmatrix} 0 & 1 & -\delta\phi \\ 1 & 0 & 0 \\ 0 & -\delta\phi & -1 \end{bmatrix}$$

where from we finally conclude

$$C_b^n(\delta\psi, \delta\theta, \delta\phi) = \begin{bmatrix} \delta\psi & 1 & -\delta\phi \\ 1 & -\delta\psi & \delta\theta \\ 0 & -\delta\phi & -1 \end{bmatrix}$$

Since

$$C_b^n(0,0,0) = \begin{bmatrix} 0 & 1 & 0 \\ 1 & 0 & 0 \\ 0 & 0 & -1 \end{bmatrix}$$

$\Rightarrow$

$$\delta C_b^n = \begin{bmatrix} \delta\psi & 0 & -\delta\phi \\ 0 & -\delta\psi & \delta\theta \\ 0 & -\delta\phi & 0 \end{bmatrix}$$

Now,

$$\begin{aligned} \delta\Psi &= -\delta C_b^n \cdot C_n^b \\ &= \begin{bmatrix} \delta\psi & 0 & -\delta\phi \\ 0 & -\delta\psi & \delta\theta \\ 0 & -\delta\phi & 0 \end{bmatrix} \begin{bmatrix} 0 & 1 & 0 \\ 1 & 0 & 0 \\ 0 & 0 & -1 \end{bmatrix} \end{aligned}$$

$\Rightarrow$

$$\delta\Psi = \begin{bmatrix} 0 & -\delta\psi & -\delta\phi \\ \delta\psi & 0 & \delta\theta \\ \delta\phi & -\delta\theta & 0 \end{bmatrix}$$

where from we calculate the "attitude error" vector

$$\delta\Psi = \begin{pmatrix} -\delta\theta \\ -\delta\phi \\ -\delta\psi \end{pmatrix}$$

Hence, the navigation state's error dynamics are

$$\frac{\delta}{\delta t}\begin{pmatrix} \delta x_n \\ \delta y_n \\ \delta z_n \\ \delta V_{xn} \\ \delta V_{yn} \\ \delta V_{zn} \\ -\delta\theta \\ -\delta\phi \\ \delta\psi \end{pmatrix} = \begin{bmatrix} 0 & 0 & 0 & 1 & 0 & 0 & 0 & 0 & 0 \\ 0 & 0 & 0 & 0 & 1 & 0 & 0 & 0 & 0 \\ 0 & 0 & 0 & 0 & 0 & 1 & 0 & 0 & 0 \\ 0 & 0 & 0 & 0 & 0 & 0 & 0 & -g & a \\ 0 & 0 & 0 & 0 & 0 & 0 & g & 0 & 0 \\ 0 & 0 & 0 & 0 & 0 & 0 & -a & 0 & 0 \\ 0 & 0 & 0 & 0 & 0 & 0 & 0 & 0 & 0 \\ 0 & 0 & 0 & 0 & 0 & 0 & 0 & 0 & 0 \\ 0 & 0 & 0 & 0 & 0 & 0 & 0 & 0 & 0 \end{bmatrix} \begin{pmatrix} \delta x_n \\ \delta y_n \\ \delta z_n \\ \delta V_{xn} \\ \delta V_{yn} \\ \delta V_{zn} \\ -\delta\theta \\ -\delta\phi \\ \delta\psi \end{pmatrix} + \begin{bmatrix} 0 & 0 & 0 & 0 & 0 & 0 \\ 0 & 0 & 0 & 0 & 0 & 0 \\ 0 & 0 & 0 & 0 & 0 & 0 \\ 0 & 1 & 0 & 0 & 0 & 0 \\ 1 & 0 & 0 & 0 & 0 & 0 \\ 0 & 0 & -1 & 0 & 0 & 0 \\ 0 & 0 & 0 & 0 & -1 & 0 \\ 0 & 0 & 0 & -1 & 0 & 0 \\ 0 & 0 & 0 & 0 & 0 & 1 \end{bmatrix} \begin{pmatrix} \delta f_x^b \\ \delta f_y^b \\ \delta f_z^b \\ \delta\omega_x^b \\ \delta\omega_y^b \\ \delta\omega_z^b \end{pmatrix} \tag{3.63}$$

3.4 Measurement Equation

From the geometry of the measurement arrangement, the "Main Equation" is obtained:

$$\begin{pmatrix} x \\ y \end{pmatrix} = \begin{pmatrix} x_p \\ y_p \end{pmatrix} - (z_p - z)\frac{1}{(0,0,1)C_b^n \begin{pmatrix} x_f \\ y_f \\ f \end{pmatrix}} \begin{bmatrix} 1 & 0 & 0 \\ 0 & 1 & 0 \end{bmatrix} C_b^n \begin{pmatrix} x_f \\ y_f \\ f \end{pmatrix} \tag{3.64}$$

For small angles:

$$C_b^n = \begin{bmatrix} \psi & 1 & -\phi \\ 1 & -\psi & \theta \\ \theta & -\phi & -1 \end{bmatrix} \tag{3.65}$$

$\Rightarrow$

$$\begin{pmatrix} x_p \\ y_p \end{pmatrix} = \begin{pmatrix} x \\ y \end{pmatrix} + (z_p - z)\frac{1}{x_f\theta - y_f\phi - f}\begin{pmatrix} x_f\psi - f\phi + y_f \\ f\theta - y_f\phi + x_f \end{pmatrix} \tag{3.66}$$

In the special case of 2-D flight, we have $y_f = 0 \Rightarrow$

$$y_p - y = \frac{z_p - z}{x_f\theta - f}(f\theta + x_f) \tag{3.67}$$

i.e.,

$$\frac{y_p - y}{z - z_p} = \frac{x_f\theta + f\theta}{f - x_f\theta} \tag{3.68}$$

Setting $\frac{f}{x_f} = \tan\zeta$ yields

$$\begin{aligned} \frac{y_p - y}{z - z_p} &= \frac{1 + tan\zeta \cdot \theta}{\tan\zeta - \theta} \\ &= \frac{1 + tan\zeta\tan\theta}{\tan\zeta - \tan\theta} \quad and\ for\ \theta \quad small \\ &= \frac{1}{\tan(\zeta - \theta)} \end{aligned}$$

$\Rightarrow$

$$\tfrac{y_p - y}{z - z_p} = \cot(\zeta - \theta),$$

as before; note the polarity of θ.

In the general 3-D case we have

$$x_p - x = (z - z_p)\frac{x_f\psi - f\phi + y_f}{f + y_f\phi - x_f\theta} \tag{3.69}$$

$$y_p - y = (z - z_p)\frac{f\theta - y_f\psi + x_f}{f + y_f\phi - x_f\theta} \tag{3.70}$$

$\Rightarrow$

$$x_p - x = (z - z_p)\frac{\frac{x_f}{f}\psi - \phi + \frac{y_f}{f}}{1 + \frac{y_f}{f}\phi - \frac{x_f}{f}\theta} \tag{3.71}$$

$$y_p - y = (z - z_p)\frac{\theta - \frac{y_f}{f}\psi + \frac{x_f}{f}}{1 + \frac{y_f}{f}\phi - \frac{x_f}{f}\theta} \tag{3.72}$$

Set

$x_p := \frac{x_p}{f}$, $y_p := \frac{y_p}{f}$

$\Rightarrow$

$$x_p - x = (z - z_p)\frac{x_f\psi - \phi + y_f}{1 + y_f\phi - x_f\theta} \tag{3.73}$$

$$y_p - y = (z - z_p)\frac{\theta - y_f\psi + x_f}{1 + y_f\phi - x_f\theta} \tag{3.74}$$

The small angles approximation yields

$$x_p - x = (z - z_p)(x_f\psi - \phi + y_f)(1 - y_f\phi + x_f\theta)$$
$$= (z - z_p)(x_f\psi - \phi + y_f - y_f^2\phi + x_f y_f\theta)$$

and

$$y_p - y = (z - z_p)(\theta - y_f\psi + x_f)(1 - y_f\phi + x_f\theta)$$
$$= (z - z_p)(\theta - y_f\psi + x_f + x_f^2\theta - x_f y_f\phi)$$

$\Rightarrow$

$$x_p - x = (z - z_p)[y_f + x_f\psi + x_f y_f\theta - (1 + y_f^2)\phi]$$

$$y_p - y = (z - z_p)[x_f - y_f\psi + (1 + x_f^2)\theta - x_f y_f\phi]$$

Thus

$$x_p - x + (z_p - z)y_f + z_p x_f\psi + z_P x_f y_f\theta - z_p(1 + y_f^2)\phi = z[x_f\psi + x_f y_f\theta - (1 + y_f^2)\phi]$$

$$y_p - y + (z_p - z)x_f + z_p y_f\psi + z_P(1 + x_f^2\theta) - z_p x_f y_f\phi = z[-y_f\psi + (1 + x_f^2)\theta - x_f y_f\phi]$$

3.4.1 Small Perturbations.

$$x = x_c - \delta x, \quad y = y_c - \delta y, \quad z = z_c - \delta z, \quad \theta = \theta_c - \delta\theta, \quad \psi = \psi_c - \delta\psi, \quad \phi = \phi_c - \delta\phi$$

Assume the position x_p, y_p, z_p of the ground feature is known.

$$x_p - x_c + \delta x + (z_p - z_c)y_f + \delta z y_f + z_p x_f \psi_c - z_p x_f y_f \delta\theta - z_p(1+y_f^2)\phi_c + z_p(1+y_f^2)\delta\phi$$

$$= z_c[x_f\psi_c - x_f\delta\psi + x_f y_f\theta_c - x_f y_f\delta\theta - (1+y_f^2)\phi_c + (1+y_f^2)\delta\phi] - \delta z[x_f\psi_c + x_f y_f\theta_c - (1+y_f^2)\phi_c]$$

$$y_p - y_c + \delta y + (z_p - z_c)x_f + \delta z x_f - z_p y_f\psi_c + z_p y_f\delta\psi + z_p(1+x_f^2)\theta_c - z_p x_f y_f\phi_c + z_p x_f y_f\delta\phi - z_p(1+x_f^2)\delta\theta$$

$$= z_c[-y_f\psi_c + y_f\delta\psi + (1+x_f^2)\theta_c - (1+x_f^2)\delta\theta - x_f y_f\phi_c + x_f y_f\delta\phi] - \delta z[y_f\psi_c + (1+x_f^2)\theta_c - x_f y_f\phi_c]$$

$$\Rightarrow$$

$$x_p - x_c + (z_p - z_c)y_f + z_p x_f\psi_c + z_p x_f y_f\theta_c - z_p(1+y_f^2)\phi_c - z_c x_f\psi_c - z_c x_f y_f\theta_c + z_c(1+y_f^2)\phi_c$$

$$= -\delta x - [x_f\psi_c + x_f y_f\theta_c - (1+y_f^2)\phi_c + y_f]\delta z + [z_p x_f y_f - z_c x_f y_f]\delta\theta + (z_c - z_p)(1+y_f^2)\delta\phi + (z_p x_f - z_c x_f)\delta\psi$$

$$y_p - y_c + (z_p - z_c)x_f - z_p y_f \psi_c + z_p(1 + x_f^2)\theta_c - z_p x_f y_f \phi_c + z_c y_f \psi_c - z_c(1 + x_f^2)\theta_c + z_c x_f y_f \phi_c$$

$$= -\delta y - [(1 + x_f^2)\theta_c - y_f \psi_c - x_f y_f \phi_c - x_f]\delta z + (1 + x_f^2)(z_p - z_c)\delta\theta + x_f y_f (z_c - z_p)\delta\phi + y_f (z_c - z_p)\delta\psi$$

$$\Rightarrow$$

$$x_p - x_c + (z_c - z_p)[(1 + y_f^2)\phi_c - x_f y_f \theta_c - x_f \psi_c - y_f] = -\delta x - [y_f + x_f \psi_c + x_f y_f \theta_c - (1 + y_f^2)\phi_c]\delta z + (z_p - z_c)[x_f y_f \delta\theta + x_f \delta\psi - (1 + y_f^2)\delta\phi]$$

$$y_p - y_c + (z_c - z_p)[y_f \psi_c - x_f y_f \psi_c - (1 + x_f^2)\theta_c - x_f] = -\delta y + [x_f + y_f \psi_c + x_f y_f \phi_c - (1 + x_f^2)\theta_c]\delta z + (z_p - z_c)[(1 + x_f^2)\delta\theta - x_f y_f \delta\phi - y_f \delta\psi]$$

On the RHS of the above two equations, set $\psi_c = \theta_c = \phi_c = 0$ (the nominal trajectory is wings level flight).

$$\Rightarrow$$

$$x_p - x_c + (z_c - z_p)[(1 + y_f^2)\phi_c - x_f y_f \theta_c - x_f \psi_c - y_f] = -\delta x - y_f \delta z + (z_p - z_c)[x_f y_f \delta\theta - (1 + y_f^2)\delta\phi + x_f \delta\psi]$$

$$y_p - y_c + (z_c - z_p)[x_f + (1 + x_f^2)\theta_c - x_f y_f \theta_c - y_f \psi_c] = -\delta y + x_f \delta z + (z_p - z_c)[(1 + x_f^2)\delta\theta - x_f y_f \delta\phi - y_f \delta\psi]$$

Also, on the RHS on the above equations, set $z_c = h$.

$$x_p - x_c + (z_c - z_p)[(1+y_f^2)\phi_c - x_f y_f \theta_c - x_f \psi_c - y_f] = -\delta x - y_f \delta z + (z_p - h)[x_f y_f \delta\theta - (1+y_f^2)\delta\phi + x_f \delta\psi]$$

$$y_p - y_c + (z_c - z_p)[x_f + (1+x_f^2)\theta_c - x_f y_f \theta_c - y_f \psi_c] = -\delta y + x_f \delta z + (z_p - h)[(1+x_f^2)\delta\theta - x_f y_f \delta\phi - y_f \delta\psi]$$

Finally, without loss of generality, assume $z_p = 0$

$$x_p - x_c + z_c[(1+y_f^2)\phi_c - x_f y_f \theta_c - x_f \psi_c - y_f] = -\delta x - y_f \delta z - h[x_f y_f \delta\theta - (1+y_f^2)\delta\phi + x_f \delta\psi]$$

$$y_p - y_c + z_c[x_f + (1+x_f^2)\theta_c - x_f y_f \theta_c - y_f \psi_c] = -\delta y + x_f \delta z - h[(1+x_f^2)\delta\theta - x_f y_f \delta\phi - y_f \delta\psi]$$

Non-dimensionalize by dividing by h:

$$x_p \to \frac{x_p}{h}, \qquad x_c \to \frac{x_c}{h}, z_c \to \frac{z_c}{h}, \qquad \delta x \to \frac{\delta x}{h}, \delta y \to \frac{\delta y}{h}, \qquad \delta z \to \frac{\delta z}{h}$$

$$x_p - x_c + z_c[y_f + x_f y_f \theta_c + x_f \psi_c - (1 + y_f^2)\phi_c] = -\delta x - y_f \delta z - x_f y_f \delta\theta$$

$$+(1 + y_f^2)\delta\phi - x_f \delta\psi$$

$$y_p - y_c + z_c[x_f + (1 + x_f^2)\theta_c - x_f y_f \theta_c - y_f \psi_c] = -\delta y + x_f \delta z - (1 + x_f^2)\delta\theta$$

$$+x_f y_f \delta\phi + y_f \delta\psi$$

$$\Rightarrow$$

In 3-D and wings level flight the measurements matrix

$$\boxed{C(t) = \begin{bmatrix} -1 & 0 & -y_f & 0 & 0 & 0 & -x_f y_f & 1 + y_f^2 & -x_f \\ 0 & -1 & x_f & 0 & 0 & 0 & -(1 + x_f^2) & x_f y_f & y_f \end{bmatrix}}$$

Note:

$$x_f = x_f(t)$$

In the special 2-D Case

$$C(t) = \begin{bmatrix} -1 & 0 & -x_f & 0 & 0 & 1 + x_f^2 \end{bmatrix} \tag{3.75}$$

as expected.

The solution method for finding the point of "Intersection" of Two Directed Straight Lines in R^3 is explained in detail in Appendix A.

IV. Results and Analysis

4.1 Development of Kalman Filtering for Flight Scenarios

State representation for flight scenarios was obtained in Chapter 3. Here we need to state discrete Kalman Filtering equations.

Sate:

$$x(k) = \Phi(k, k-1)x(k-1) + B(k-1)u(k-1) + G(w(k-1)) \tag{4.1}$$

Measurement:

$$Z(k) = H(k)x(k) + V(k) \tag{4.2}$$

Propagation:

$$\hat{x}^-(k) = \Phi(k, k-1)\hat{x}^+(k-1) \tag{4.3}$$

$$P^-(k) = \Phi(k, k-1)P^+(k-1)\Phi(k, k-1)^T + GQG^T \tag{4.4}$$

Update:

$$K(k) = P^-(k)H^T(k)[H(k)P^-(k)H^T(k) + R(k)]^{-1} \tag{4.5}$$

$$\hat{x}^+(k) = \hat{x}^-(k) + K(k)[Z(k) - H(k)\hat{x}^-(k)] \tag{4.6}$$

$$P^+(k) = P^-(k) - K(k)H(k)P^-(k) \tag{4.7}$$

4.2 Scenario 1

Here in this case we have almost perfect level flight in 3 - D. Euler angles are assumed negligible. Accelerometers of the INS have bias $0.01 m/s^2$, initial state estimate and covariance are set as random, and measurement and also position of the UAV calculated based on measurement assumed perfect. Here we have 1 m/s^2 constant acceleration in y direction (North). Flight level is 500 meters. 16 objects are generated randomly. Ten measurements are obtained. In this scenario we tried algorithm for one object per measurement. Positions of ground objects are assumed known. Error plots from Kalman filter are shown below, and all other plots are placed in Appendix B.

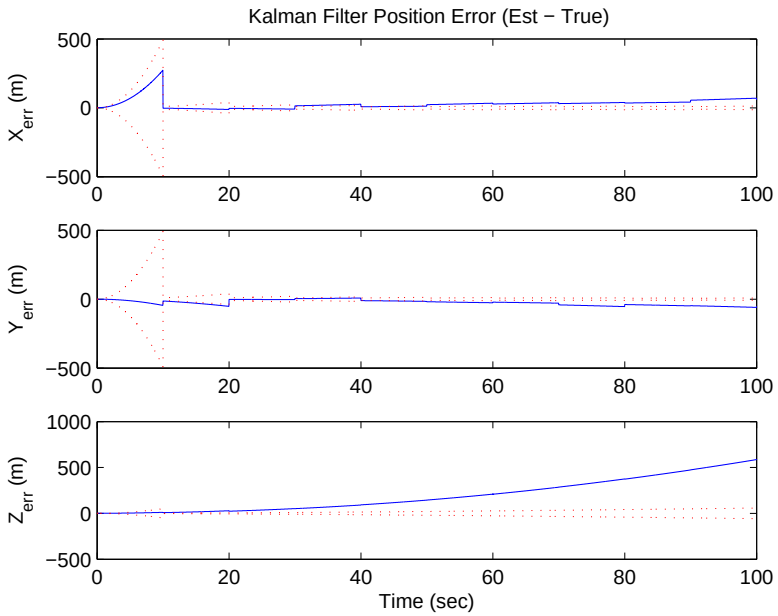

Figure 4.1: Scenario 1. Kalman Filter Position Errors. Estimated - true. Red is +− standard deviation.

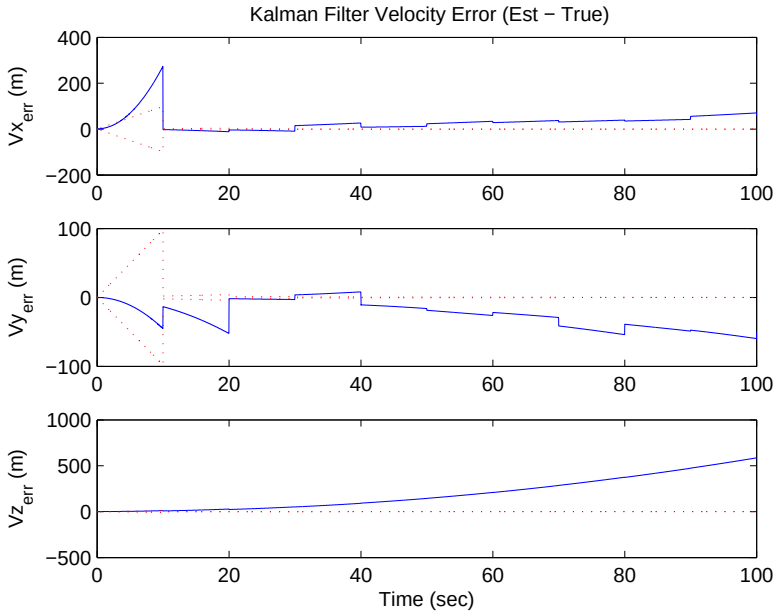

Figure 4.2: Scenario 1. Kalman Filter Velocity Errors. Estimated - true. Red is +− standard deviation.

Table 4.1: Standard deviation results obtained from Kalman filtering of scenario 1.

Standard Deviation	Value
σ_x	28.3415 (m)
σ_y	26.7456 (m)
σ_z	24.8587 (m)
σ_{vx}	5.8403 (m/s)
σ_{vy}	5.5674 (m/s)
σ_{vz}	1.1592 (m/s)
σ_θ	0.1031 (rad)
σ_ϕ	0.1916 (rad)
σ_ψ	0.9892 (rad)

4.3 Scenario 2

Here in this scenario we have almost same conditions. Euler angles are assumed negligible. Accelerometers of the INS have bias $0.01 m/s^2$, initial state estimate and covariance are set as random, and measurement and also position of the UAV calculated based on measurement assumed perfect. Here we have 1 m/s^2 constant acceleration in y direction (North). Flight level is 500 meters. 16 objects are generated randomly. Ten measurements are obtained. In this scenario we tried algorithm for two object per measurement. Positions of ground objects are assumed known. Error plots from Kalman filter are shown below, and all other plots are placed in Appendix C.

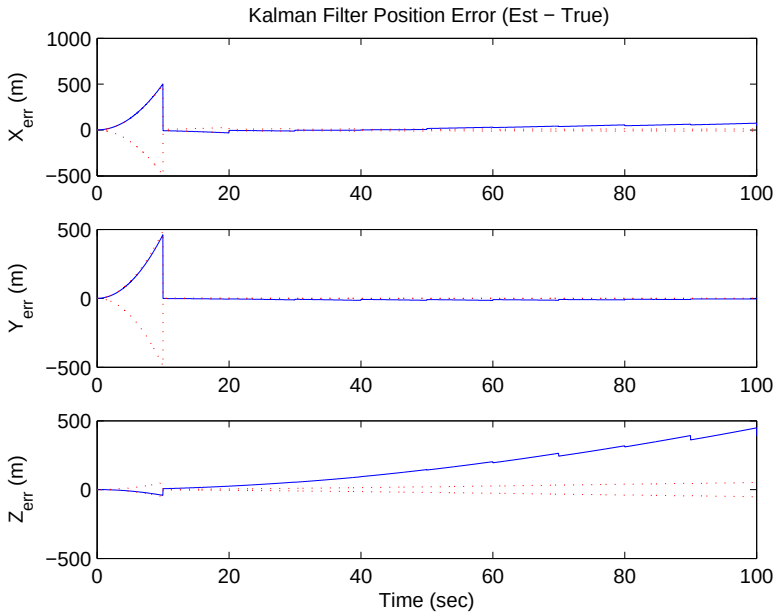

Figure 4.3: Scenario 2. Kalman Filter Position Errors. Estimated - true. Red is +− standard deviation.

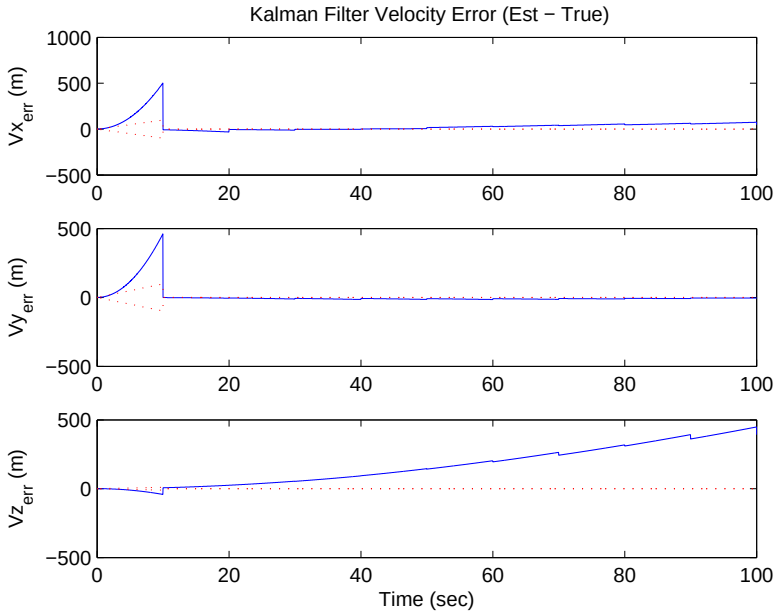

Figure 4.4: Scenario 2. Kalman Filter Velocity Errors. Estimated - true. Red is +− standard deviation.

Table 4.2: Standard deviation results obtained from Kalman filtering of scenario 2.

Standard Deviation	Value
σ_x	26.0850 (m)
σ_y	17.5229 (m)
σ_z	23.7029 (m)
σ_{vx}	5.6905 (m/s)
σ_{vy}	4.9955 (m/s)
σ_{vz}	1.1419 (m/s)
σ_θ	0.1005 (rad)
σ_ϕ	0.1845 (rad)
σ_ψ	0.9216 (rad)

4.4 Scenario 3

Same conditions applied in this scenario for three ground objects. Euler angles are assumed negligible. Accelerometers of the INS have bias $0.01 m/s^2$, initial state estimate and covariance are set as random, and measurement and also position of the UAV calculated based on measurement assumed perfect. Here we have 1 m/s^2 constant acceleration in y direction (North). Flight level is 500 meters. 16 objects are generated randomly. Ten measurements are obtained. In this scenario we tried algorithm for three object per measurement. Positions of ground objects are assumed known. Error plots from Kalman filter are shown below, and all other plots are placed in Appendix D.

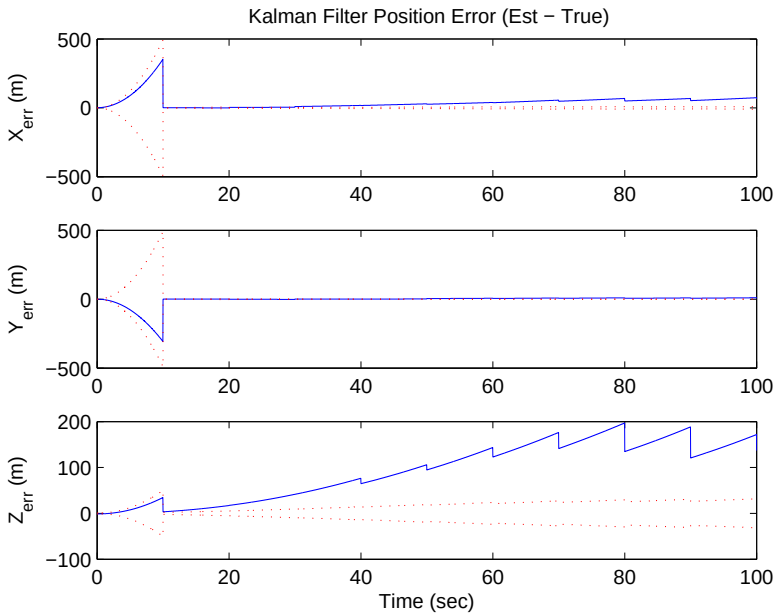

Figure 4.5: Scenario 3. Kalman Filter Position Errors. Estimated - true. Red is +− standard deviation.

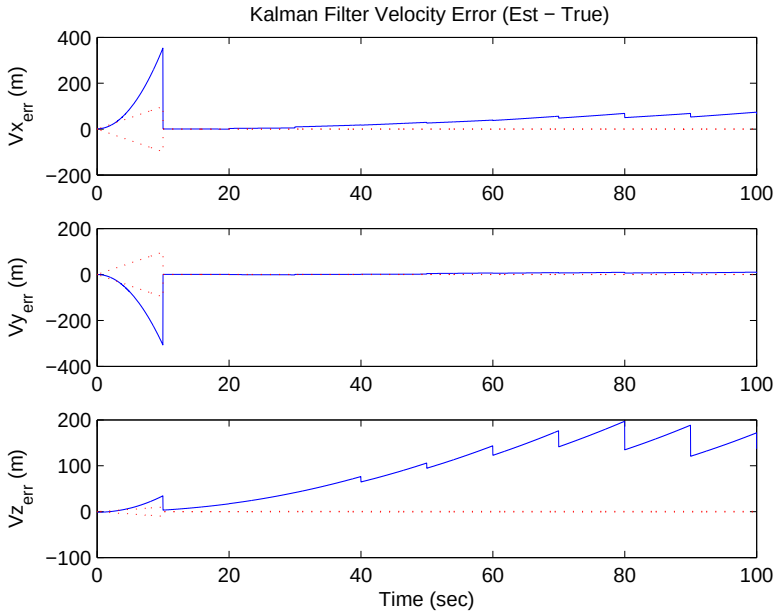

Figure 4.6: Scenario 3. Kalman Filter Velocity Errors. Estimated - true. Red is +− standard deviation.

Table 4.3: Standard deviation results obtained from Kalman filtering of scenario 3.

Standard Deviation	Value
σ_x	21.7347 (m)
σ_y	17.2366 (m)
σ_z	18.4061 (m)
σ_{vx}	5.3178 (m/s)
σ_{vy}	4.9784 (m/s)
σ_{vz}	1.0640 (m/s)
σ_θ	0.1004 (rad)
σ_ϕ	0.1841 (rad)
σ_ψ	0.9264 (rad)

4.5 Scenario 4

Here in this scenario we repeated conditions for two objects like in scenario 2. Positions of object reflection on the camera scene were obtained as in previous scenarios. Then this information was used as input for the methodology explained in Appendix A. Measured object positions are very different at third dimension z. This could be because of non-dimentialisation used in our methodology. We used input from barometric altimeter to correct this error. Firstly we ran Kalman filter for perfect measurement. Then we replaced perfect measurements with measurement of our algorithm, and we ran Kalman filter again to compare results. Plots for both runs are shown below.

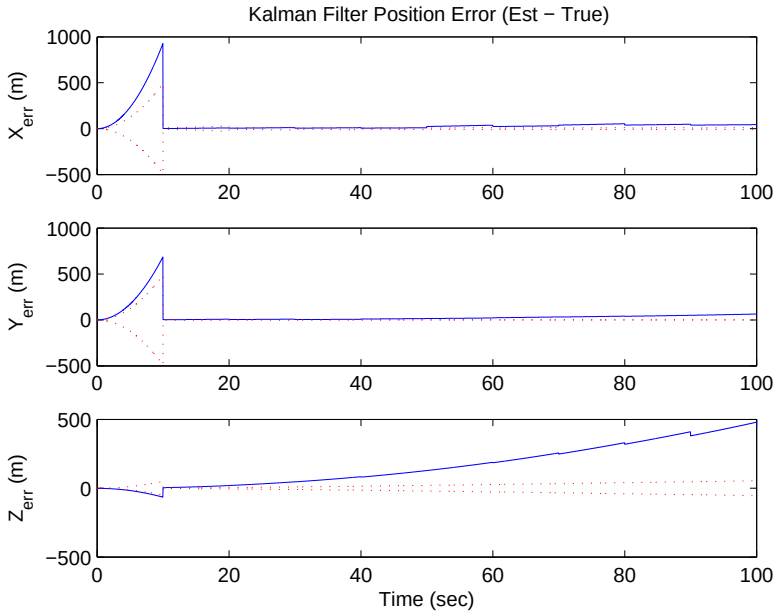

Figure 4.7: Scenario 4. Kalman Filter Results from Perfect Measurement. Kalman Filter Position Errors. Estimated - true. Red is +− standard deviation.

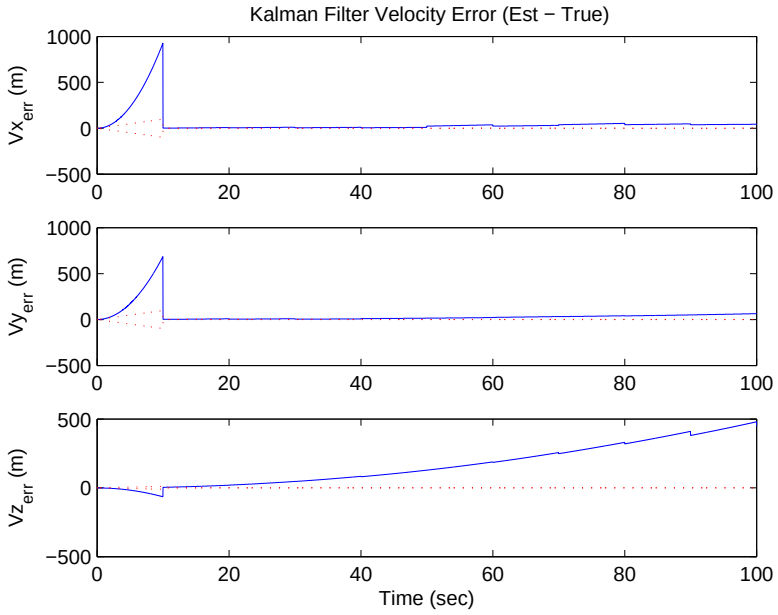

Figure 4.8: Scenario 4. Kalman Filter Results from Perfect Measurement. Kalman Filter Velocity Errors. Estimated - true. Red is +− standard deviation.

Table 4.4: Standard deviation results obtained from Kalman filtering of scenario 4.

Standard Deviation	Value
σ_x	25.3797 (m)
σ_y	17.5103 (m)
σ_z	24.0239 (m)
σ_{vx}	5.6623 (m/s)
σ_{vy}	4.9949 (m/s)
σ_{vz}	1.1304 (m/s)
σ_θ	0.1005 (rad)
σ_ϕ	0.1892 (rad)
σ_ψ	0.9849 (rad)

Table 4.5: Calculated object positions for Scenario4.

x	-0.0018	-0.0024	-0.0015	-0.0010	-0.0271	-0.0442	0.0246	0.1971	0.2699
y	125	325	625.02	1025.1	1525.2	2125.6	2826.4	3628.6	4533.1
z	0.0000	0.0000	0.0000	0.0001	0.0001	0.0002	0.0004	0.0006	0.0010

Table 4.6: Barometric altimeter added object positions for Scenario4.

x	-0.0018	-0.0024	-0.0015	-0.0010	-0.0271	-0.0442	0.0246	0.1971	0.2699
y	125	325	625.02	1025.1	1525.2	2125.6	2826.4	3628.6	4533.1
z	-500	-500	-500	-499.9	-499.9	-499.8	-499.6	-499.4	-499

Table 4.7: True object positions for Scenario4.

x	-0.1388	-0.1360	-0.0262	-0.0083	-0.1158	-0.0988	0.0332	0.1551	0.1355
y	213.5	330.3	752.1	1315.7	2063.0	3142.3	4376.4	6006.0	8105.4
z	-493.5	-490.4	-491.2	-494.3	-494.1	-499.5	-499.2	-490.1	-497.5

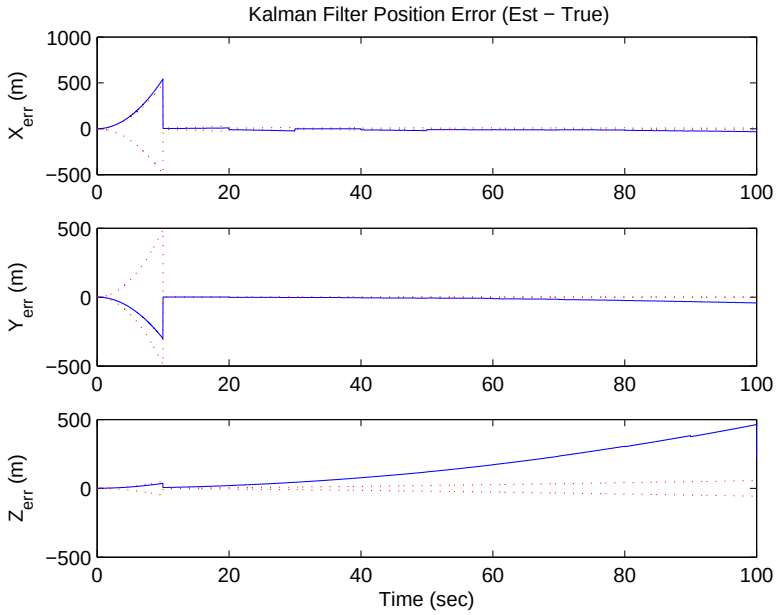

Figure 4.9: Scenario 4. Kalman Filter Position Errors after Least Square Method Applied. Estimated - true. Red is +− standard deviation.

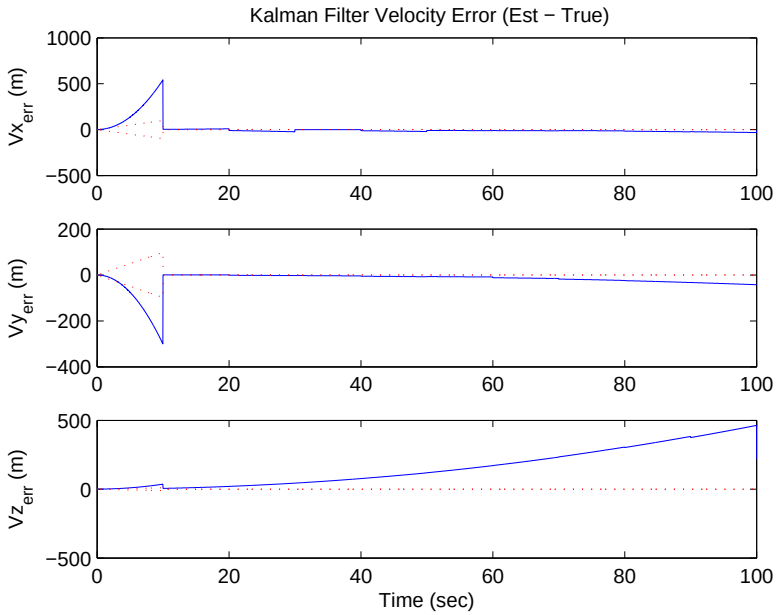

Figure 4.10: Scenario 4. Kalman Filter Velocity Errors after Least Square Method Applied. Estimated - true. Red is +− standard deviation.

Table 4.8: Scenario 4. Standard deviation results obtained from Kalman filtering after Least Square Method Applied.

Standard Deviation	Value
σ_x	24.92 (m)
σ_y	17.488 (m)
σ_z	24.668 (m)
σ_{vx}	5.6601 (m/s)
σ_{vy}	4.9942 (m/s)
σ_{vz}	1.1479 (m/s)
σ_θ	0.10047 (rad)
σ_ϕ	0.19122 (rad)
σ_ψ	0.98697 (rad)

Table 4.9: Standard deviation results obtained from Kalman filtering of Scenario1, Scenario2, and Scenario3.

Std	Scenario1	Scenario2	Scenario3
σ_x	28.3415 (m)	26.0850 (m)	21.7347 (m)
σ_y	26.7456 (m)	17.5229 (m)	17.2366 (m)
σ_z	24.8587 (m)	23.7029 (m)	18.4061 (m)
σ_{vx}	5.8403 (m/s)	5.6905 (m/s)	5.3178 (m/s)
σ_{vy}	5.5674 (m/s)	4.9955 (m/s)	4.9784 (m/s)
σ_{vz}	1.1592 (m/s)	1.1419 (m/s)	1.0640 (m/s)
σ_θ	0.1031 (rad)	0.1005 (rad)	0.1004 (rad)
σ_ϕ	0.1916 (rad)	0.1845 (rad)	0.1841 (rad)
σ_ψ	0.9892 (rad)	0.9216 (rad)	0.9264 (rad)

4.6 Analysis

We need to compare plot results and statistics before state our conclusion. Look at the table that shows statistical results for first three scenarios above. It is obvious that we have smaller standard deviations when we have more tracked objects. If we look at the error plots for scenarios, we can see that the worst one is the first scenario where we have one object tracked, and third scenario looks better than first and second. Results for second scenario are better than first. However, comparing plots and statistics we expected to see impact of using two or more tracked object to prove the claim very clearly. Even that second scenario has better results in comparing with first one, difference between them is not significant. There were unexpected error grows in z direction. The theory explained in Chapter 3 gives us measurement update for x and y positions, and as investigated in scenario 4 we need to have barometric altimeter aid. Results could be improved by tuning filter more accurately, and that requires further study on scenarios and code.

V. Conclusions

5.1 Conclusion

In the first step of this study the simplest 2-D scenario of INS aiding using bearing measurements of stationary ground features is investigated. The measurements are taken over time and the attendant observability problem is formulated and analyzed. The degree of INS aiding action is determined by the degree of observability provided by the measurement arrangement. The latter is strongly influenced by the nature of the available measurements - in our case, bearing measurements of stationary ground objects - the trajectory of the aircraft, and the length of the measurement interval. Whereas observability guarantees that all the navigation state's components are positively affected by the external measurements, we are also interested in the possibility of partial observability where not all the navigation state components' estimates are impacted by the external measurements. It is shown that when one known ground object is tracked, the observability Grammian is rank deficient and thus full INS aiding action is not available. However, if baro altitude is available and an additional vertical gyroscope is used to provide an independent measurement of the aircraft's pitch angle, a data driven estimate of the complete navigation state can be obtained. If two ground features are simultaneously tracked the observability Grammian is full rank and all the components of the navigation state vector are positively impacted by the optical measurements. The simulation we applied here do not fully validate the theory and there full further work is needed.

In the second step of this study simple scenario for 3-D flight and INS aiding using bearing measurements of stationary ground features is investigated. Ground objects are generated and measurements are obtained using those ground objects. In the scenarios, one ground object tracking, two ground objects tracking, and three ground objects tracking investigated. Having more ground objects provided some better results, and also smaller standard deviations. In theory and in application we note that each measured position of the aircraft, which also refers to an image taken by the camera, is related to two ground object such that are common in two neighbor

images. In situation to have less than two matched ground objects/features INS propagation will continue, however measurement propagation chain, showed in Chapter four Scenario 2, will be crashed. Three ground objects are necessary to initialize the process only. After that point, first two good measurements would be set as new initial condition, and that will be the second start point for measurement propagation. Measurements iterations after that can be assumed as good relative to that second start point. Some other measurement input or method would be essential to obtain geometric/geodetic relation between last good measurement of first chain and first good measurement of last chain.

5.2 Next Iterations

Here we have some recommendations for further studies.

• Euler angles are assumed small in this study. One can extend the study using second terms of Taylor series of sine and cosine. After that some nonlinear methods or extended linearisation would be essential.

• This study was designed to be a part of control and navigation system, that consists of image processing block upfront, Kalman Filter for navigation solution, LQG flight controller, communication system, weapon systems and other subsystems. Those who work on manual target selection might use algorithm in this study to obtain geo-location of selected target. Then it is easy to obtain relative distance to the selected target, so one can consider to give inputs to approach closer to the selected target or fly away from it. It could be done either manually or a simple algorithm that has those two options could be adopted to the LQG controller.

• Those, who do research about flight patterns to observe possible enemies, to protect moving friendly troopers, could extend their research for patterns also to fly

over gaps where measurement propagation chains are broken, explained at the end of conclusions, to obtain new and useful measurement information. That would be useful to connect separate chains.

Appendix A. The Point of "Intersection" of Two Directed Straight Lines in R^3

The two straight lines are

$$l_1 = \{P|P = P_1 + tV_1, t \geq 0\}$$

$$l_2 = \{P|P = P_2 + tV_2, t \geq 0\}$$

The lines' "points of origin" are P_1 and P_2, respectively. V_1 and V_2 are unit vectors in R^3.

Lemma1 The distance $d(P, l)$ from a specified point P to the straight line

$$l_1 = \{P|P = P_1 + tV_1, t \geq 0\}$$

is

$$d = \left\{ \begin{array}{cc} ||P - P_1||_2 & if \quad V_1^T(P - P_1) \leqslant 0 \\ \sqrt{||P - P_1||_2^2 - (P - P_1)^T V V^T (P - P_1)} & if \quad V_1^T(P - P_1) \geq 0 \end{array} \right\}$$

Proof: Solve the optimization problem

$$min_{t \epsilon \Re_t^1} (P_1 - P + tV)^T (P_1 - P + tV)$$

We obtain

$$\boxed{t^* = V^T(P - P_1)} \ \square$$

wherupon we calculate d.

The point of "intersection" P of two straight lines in $\Re^3$ is such that:

$$d^2(P, l_1) + d^2(P, l_2) \rightarrow min;$$

We have evoked the "least squares" principle.

Thus, the optimization problem is posed.

$$min_{P\epsilon\Re^3}[d^2(P,l_1)+d^2(P,l_2)]$$

From Lemma 1 we conclude:

$$min_{P\epsilon\Re^3}[(P-P_1)^T(P-P_1)-(P-P_1)^TV_1V_1^T(P-P_1)+(P-P_2)^T(P-P_2)-(P-P_2)^TV_2V_2^T(P-P_2)]$$

$\Rightarrow$

$$P-P_1-V_1V_1^T(P-P_1)+P-P_2-V_2V_2^T(P-P_2)=0$$

$\Rightarrow$

$$P^*=\frac{1}{2}[I_3-\frac{1}{2}(V_1V_1^T+V_2V_2^T)]^{-1}\cdot[P_1+P_2-(V_1V_1^TP_1+V_2V_2^TP_2) \quad \text{(A.1)}$$

providet that:

$$V_1^T[I-frac12(V_1V_1^T+V_2V_2^T)]^{-1}[P_1+P_2-(V_1V_1^TP_1+V_2V_2^TP_2)]\geq 2V_1^TP_1 \quad \text{(A.2)}$$

and

$$V_2^T[I-frac12(V_1V_1^T+V_2V_2^T)]^{-1}[P_1+P_2-(V_1V_1^TP_1+V_2V_2^TP_2)]\geq 2V_2^TP_2 \quad \text{(A.3)}$$

The geometry is illustrated in Figure A.1:

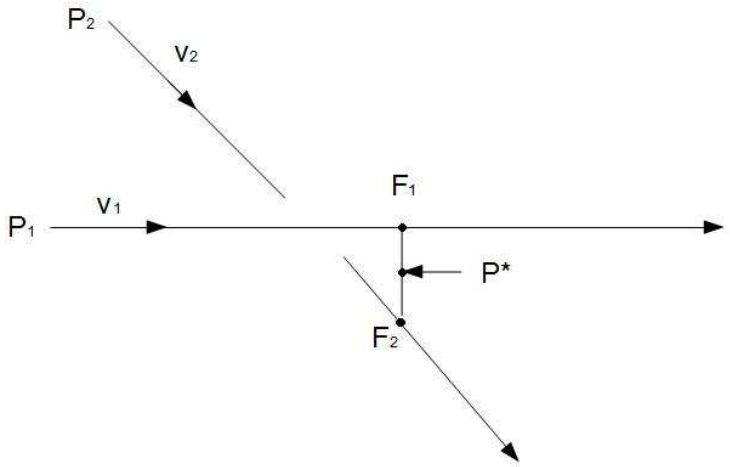

Figure A.1: Crossing lines

From Lemma 1 we know

$$t_1^* = V_1^T(P^* - P_1) \; and \; t_2^* = V_2^T(P^* - P_2)$$

wherefrom we calculate

$$F_1 = P_1 + V_1V_1^T(P^* - P_1) \; and \; F_2 = P_2 + V_2V_2^T(P^* - P_2)$$

Next calculate

$$X \equiv \tfrac{1}{2}(F_1 + F_2)$$

$$X = \frac{1}{2}[P_1 + P_2 - (V_1V_1^TP_1 + V_2V_2^TP_2) + (V_1V_1^T + V_2V_2^T)P^*] \tag{A.4}$$

From eq (A.1) we obtain

$$P_1 + P_2 - (V_1V_1^TP_1 + V_2V_2^TP_2) = 2[I - frac12(V_1V_1^T + V_2V_2^T)]P^* \tag{A.5}$$

Inserting eq (A.5) into eq (A.4) yields

$$X = \tfrac{1}{2}[2I - (V_1V_1^T + V_2V_2^T) + (V_1V_1^T + V_2V_2^T)]P^*$$

$\Rightarrow$

$$X = P^*$$

We conclude:

The point of "intersection" of the straight lines l_1 and l_2 is the midpoint of a segment $\overline{F_1F_2}$ where $F_1 \,\epsilon\, l_1$, $F_2 \,\epsilon\, l_2$, and the segment $\overline{F_1F_2}$ is otrhogonal to both l_1 and l_2. Finally, $\overline{F_1F_2} = min_{F_1 \epsilon l_1, F_2 \epsilon l_2} d(\overline{F_1F_2})$.

This characterization of the "intersection" P^* of the staright lines l_1 and l_2 yields the following alternative algorithm for the calculation of P^*.

$$F_1 = P_1 + V_1t_1, \qquad\qquad F_2 = P_2 + V_2t_2$$

$\Rightarrow$

$$F_1 - F_2 = P_1 - P_2 + V_1t_1 - V_2t_2$$

Now $V_1^T(F_1 - F_2) = 0$ and $V_2^T(F_1 - F_2) = 0$

and this yields the two equations in the unknown t_1 and t_2

$$V_1^T(P_1 - P_2 + V_1t_1 - V_2t_2) = 0$$

$$V_2^T(P_1 - P_2 + V_1t_1 - V_2t_2) = 0$$

$\Rightarrow$

$$\begin{bmatrix} 1 & -V_1^TV_2 \\ V_2^TV_1 & -1 \end{bmatrix} \begin{pmatrix} t_1 \\ t_2 \end{pmatrix} = \begin{bmatrix} V_1^T(P_2 - P_1) \\ V_1^T(P_2 - P_1) \end{bmatrix}$$

$\Rightarrow$

$$\begin{pmatrix} t_1 \\ t_2 \end{pmatrix} = \frac{1}{(V_1^T V_2)^2 - 1} \begin{bmatrix} 1 & -V_1^T V_2 \\ V_2^T V_1 & -1 \end{bmatrix} \begin{bmatrix} V_1^T (P_2 - P_1) \\ V_1^T (P_2 - P_1) \end{bmatrix}$$

$\Rightarrow$

$$t_1^* = \frac{1}{(V_1^T V_2)^2 - 1} V_1^T [I - V_2 V_2^T](P_1 - P_2)$$

$$t_2^* = \frac{1}{(V_1^T V_2)^2 - 1} V_2^T [I - V_1 V_1^T](P_2 - P_1)$$

$\Rightarrow$

$$F_1 = P_1 + \frac{1}{(V_1^T V_2)^2 - 1} V_1 V_1^T [I - V_2 V_2^T](P_1 - P_2)$$

$$F_2 = P_2 + \frac{1}{(V_1^T V_2)^2 - 1} V_2 V_2^T [I - V_1 V_1^T](P_2 - P_1)$$

$\Rightarrow$

$$P^* = \frac{1}{2}\{P_1 + P_2 + \frac{1}{(V_1^T V_2)^2 - 1}[V_1 V_1^T - V_2 V_2^T + V_2 V_2^T V_1 V_1^T - V_1 V_1^T V_2 V_2^T](P_1 - P_2)\}$$

$$P^* = \frac{1}{2}\{P_1 + P_2 + \frac{1}{(V_1^T V_2)^2 - 1}[V_1 V_1^T - V_2 V_2^T + V_1 V_2^T (V_2 V_1^T - V_1 V_2^T)](P_1 - P_2)\}$$

A 3×3 matrix inversion is not required.

If

$$V_1^T [I - \frac{1}{2}(V_1 V_1^T + V_2 V_2^T)]^{-1} [P_1 + P_2 - (V_1 V_1^T P_1 + V_2 V_2^T P_2)] \leq 2 V_1^T P_1$$

$$V_2^T [I - \frac{1}{2}(V_1 V_1^T + V_2 V_2^T)]^{-1} [P_1 + P_2 - (V_1 V_1^T P_1 + V_2 V_2^T P_2)] \leq 2 V_2^T P_2$$

then

$$t_1^* = t_2^* = 0$$

and

$$P^* = \tfrac{1}{2}(P_1 + P_2)$$

The situation is:

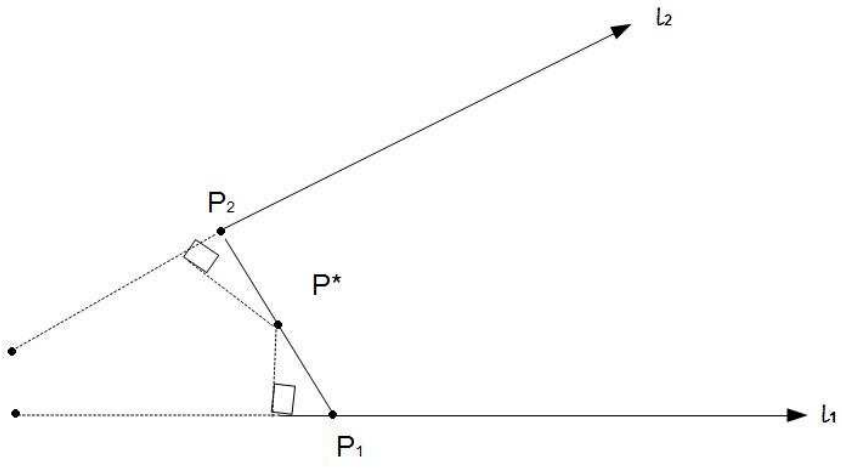

Figure A.2: $P*$ is the point in the middle of the shortest distance between l_1 and l_2

If

$$V_1^T[I - \tfrac{1}{2}(V_1V_1^T + V_2V_2^T)]^{-1}[P_1 + P_2 - (V_1V_1^TP_1 + V_2V_2^TP_2)] \geq 2V_1^TP_1$$

but

$$V_2^T[I - \tfrac{1}{2}(V_1V_1^T + V_2V_2^T)]^{-1}[P_1 + P_2 - (V_1V_1^TP_1 + V_2V_2^TP_2)] \leq 2V_2^TP_2$$

The situation is:

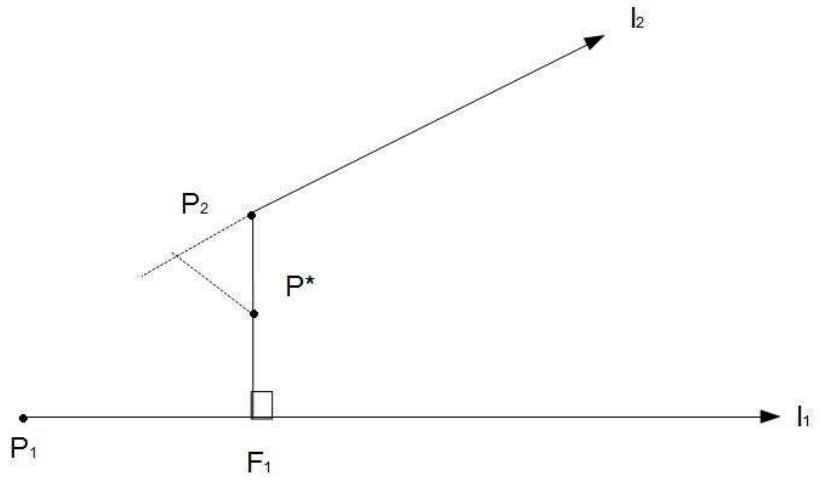

Figure A.3:

Using Lemma 1 we obtain

$$t_1^* = V_1^T(P_2 - P_1) \Rightarrow F_1 = P_1 + V_1V_1^T(P_2 - P_1)$$

$\Rightarrow$

$$\boxed{P^* = \tfrac{1}{2}[P_1 + P_2 - V_1V_1^T(P_1 - P_2)]}$$

In summary, the following holds

Theorem 2 The point of "intersection" of the straight lines $l_1 = \{P|P = P_1 + tV_1, t \geq 0\}$ *and* $l_2 = \{P|P = P_2 + tV_2, t \geq 0\}$ is calculated as follows.

If the problem parameters satisfy

$$V_1^T[I - \tfrac{1}{2}(V_1V_1^T + V_2V_2^T)]^{-1}[P_1 + P_2 - (V_1V_1^TP_1 + V_2V_2^TP_2)] \geq 2V_1^TP_1$$

and

$$V_2^T[I - \tfrac{1}{2}(V_1V_1^T + V_2V_2^T)]^{-1}[P_1 + P_2 - (V_1V_1^TP_1 + V_2V_2^TP_2)] \geq 2V_2^TP_2$$

The point of "intersection" of the straight lines l_1 and l_2 is

$$P^* = \tfrac{1}{2}[I - \tfrac{1}{2}(V_1V_1^T + V_2V_2^T)]^{-1} \cdot [P_1 + P_2 - (V_1V_1^TP_1 + V_2V_2^TP_2)]$$

An alternative formula is:

$$P^* = \tfrac{1}{2}\{P_1 + P_2 + \tfrac{1}{(V_1^TV_2)^2-1}[V_1V_1^T - V_2V_2^T + V_1V_2^T(V_2V_1^T - V_1V_2^T)](P_1 - P_2)\}$$

If the parameters are such that:

$$V_1^T[I - \tfrac{1}{2}(V_1V_1^T + V_2V_2^T)]^{-1}[P_1 + P_2 - (V_1V_1^TP_1 + V_2V_2^TP_2)] \leq 2V_1^TP_1$$

and

$$V_2^T[I - \tfrac{1}{2}(V_1V_1^T + V_2V_2^T)]^{-1}[P_1 + P_2 - (V_1V_1^TP_1 + V_2V_2^TP_2)] \leq 2V_2^TP_2$$

then

$$P^* = \tfrac{1}{2}(P_1 + P_2)$$

If the problem parameters are such that:

$$V_1^T[I - \tfrac{1}{2}(V_1V_1^T + V_2V_2^T)]^{-1}[P_1 + P_2 - (V_1V_1^TP_1 + V_2V_2^TP_2)] \geq 2V_1^TP_1$$

and

$$V_2^T[I - \tfrac{1}{2}(V_1V_1^T + V_2V_2^T)]^{-1}[P_1 + P_2 - (V_1V_1^TP_1 + V_2V_2^TP_2)] \leq 2V_2^TP_2$$

Then

$$P^* = \tfrac{1}{2}[P_1 + P_2 - V_1V_1^T(P_1 - P_2)]$$

If the problem parameters are such that:

$$V_1^T[I - \tfrac{1}{2}(V_1V_1^T + V_2V_2^T)]^{-1}[P_1 + P_2 - (V_1V_1^TP_1 + V_2V_2^TP_2)] \leq 2V_1^TP_1$$

and

$$V_2^T[I - \tfrac{1}{2}(V_1V_1^T + V_2V_2^T)]^{-1}[P_1 + P_2 - (V_1V_1^TP_1 + V_2V_2^TP_2)] \geq 2V_2^TP_2$$

then

$$\boxed{P^* = \tfrac{1}{2}[P_1 + P_2 - V_2V_2^T(P_1 - P_2)]} \ \square$$

Appendix B. Plots for Scenario 1

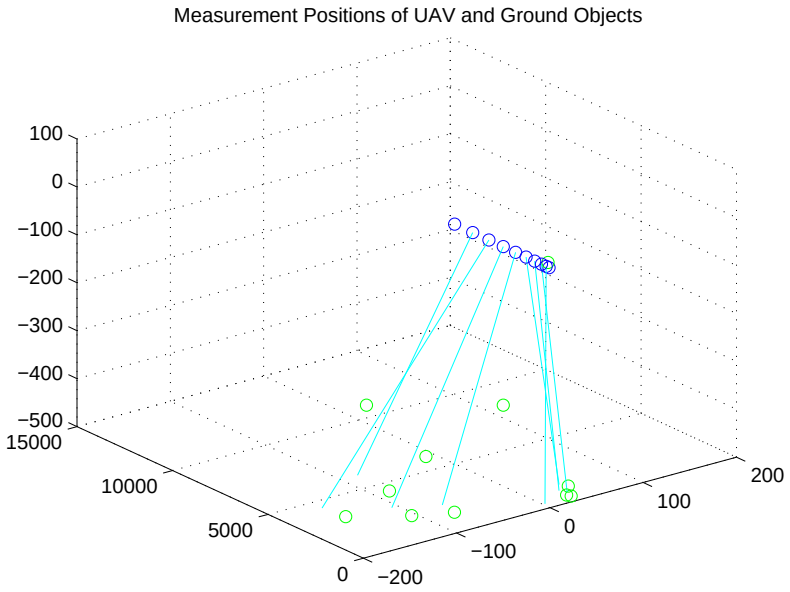

Figure B.1: Scenario 1. Simulated positions of the UAV and ground objects.

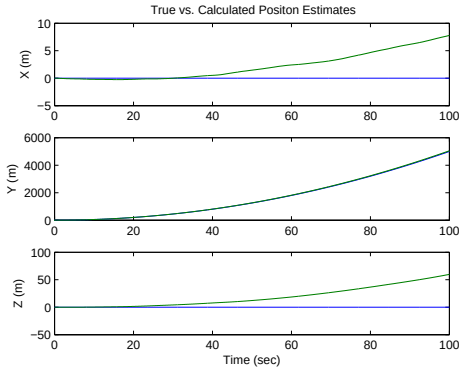

Figure B.2: Scenario 1. True vs calculated position.

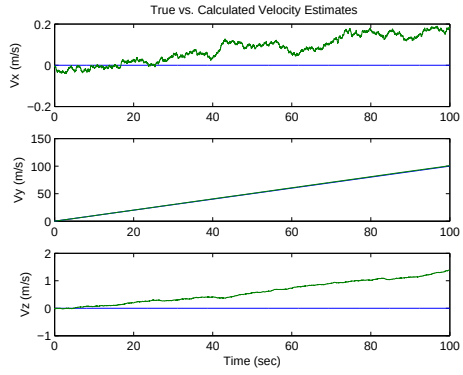

Figure B.3: Scenario 1. True vs calculated velocity.

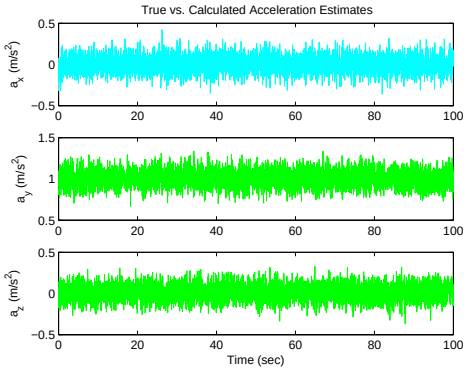

Figure B.4: Scenario 1. True vs calculated acceleration.

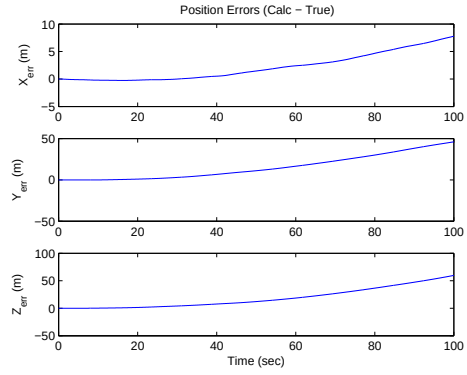

Figure B.5: Scenario 1. Position errors.

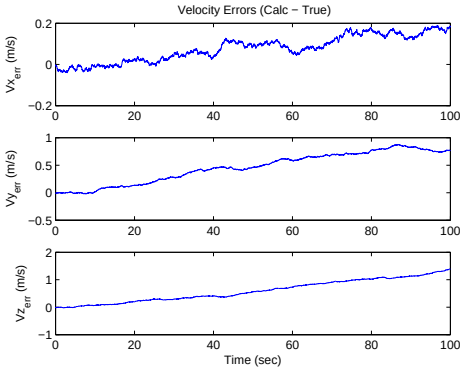

Figure B.6: Scenario 1. Velocity errors.

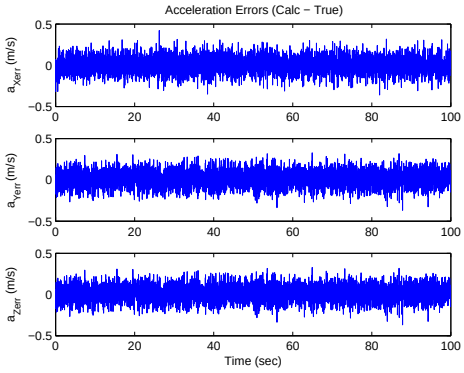

Figure B.7: Scenario 1. Acceleration errors.

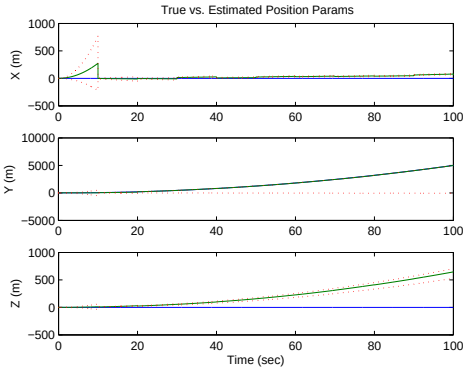

Figure B.8: Scenario 1. Kalman Filter True vs Estimated Position Parameters. Red is +− standart deviation. Blue - true, green -estimated.

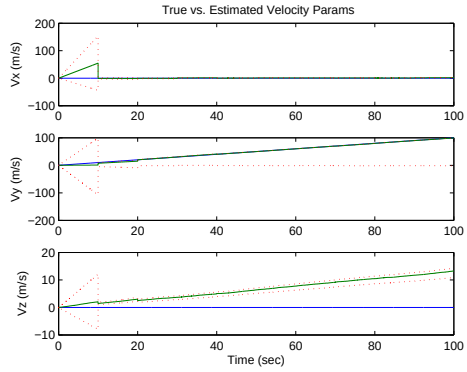

Figure B.9: Scenario 1. Kalman Filter True vs estimated Velocity Parameters. Red is +− standart deviation. Blue - true, green -estimated.

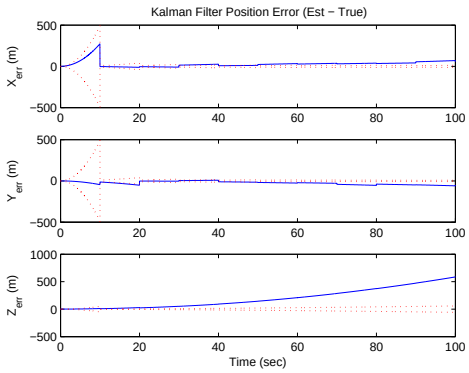

Figure B.10: Scenario 1. Kalman Filter Position Errorts. Estimated - true. Red is +− standart deviation.

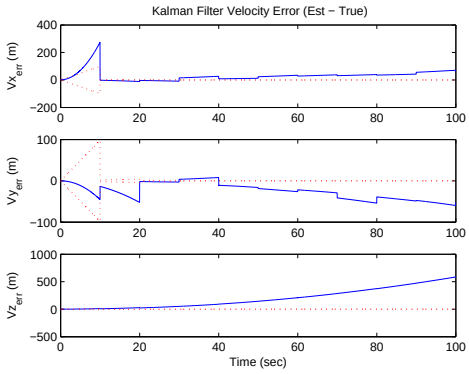

Figure B.11: Scenario 1. Kalman Filter Velocity Errorts. Estimated - true. Red is +− standart deviation.

Appendix C. Plots for Scenario 2

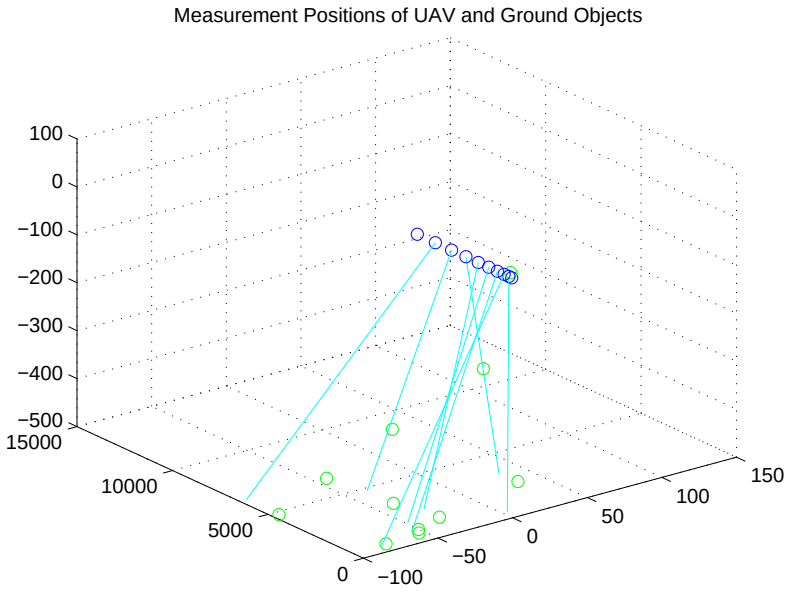

Figure C.1: Scenario 2. Simulated positions of the UAV and ground objects.

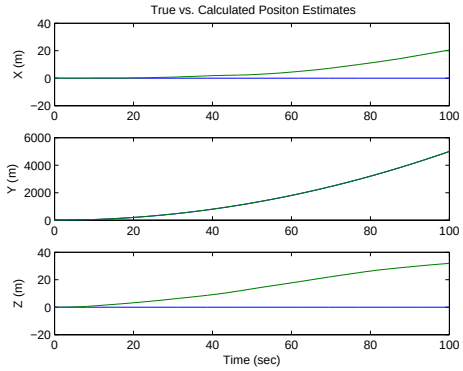

Figure C.2: Scenario 2. True vs calculated position.

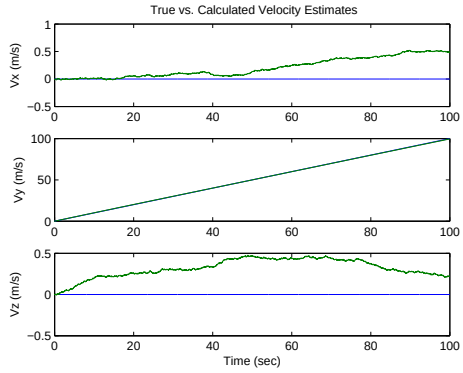

Figure C.3: Scenario 2. True vs calculated velocity.

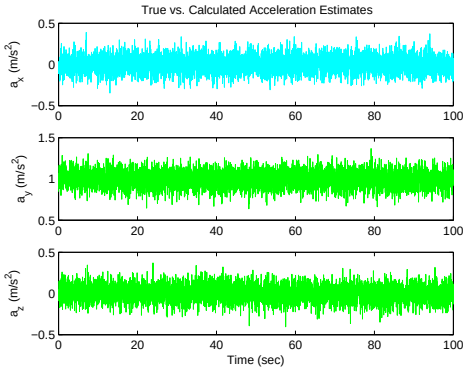

Figure C.4: Scenario 2. True vs calculated acceleration.

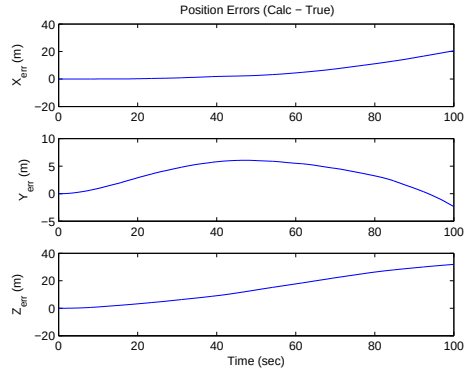

Figure C.5: Scenario 2. Position errors.

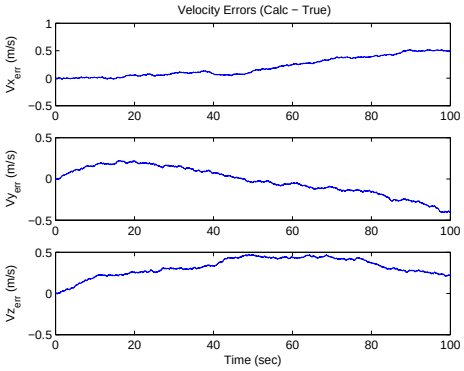

Figure C.6: Scenario 2. Velocity errors.

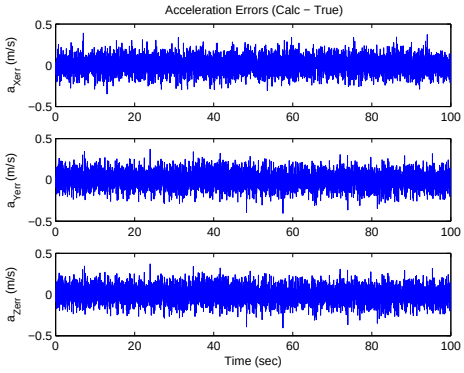

Figure C.7: Scenario 2. Acceleration errors.

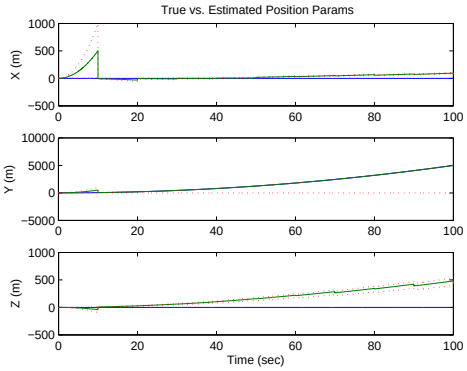

Figure C.8: Scenario 2. Kalman Filter True vs Estimated Position Parameters. Red is +− standart deviation. Blue - true, green -estimated.

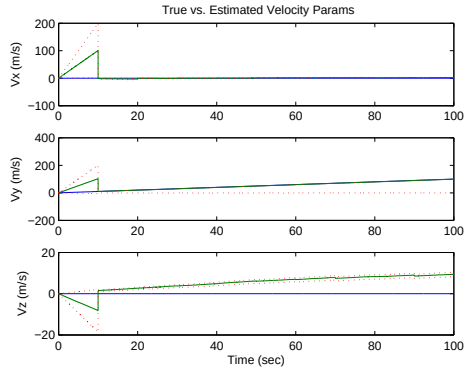

Figure C.9: Scenario 2. Kalman Filter True vs estimated Velocity Parameters. Red is +− standart deviation. Blue - true, green -estimated.

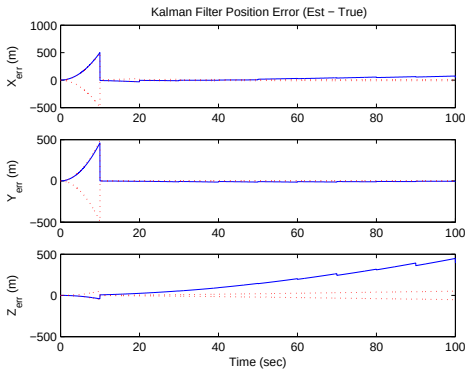

Figure C.10: Scenario 2. Kalman Filter Position Errorts. Estimated - true. Red is +− standart deviation.

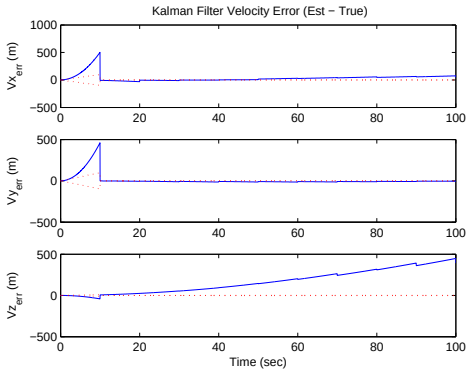

Figure C.11: Scenario 2. Kalman Filter Velocity Errorts. Estimated - true. Red is +− standart deviation.

Appendix D. Plots for Scenario 3

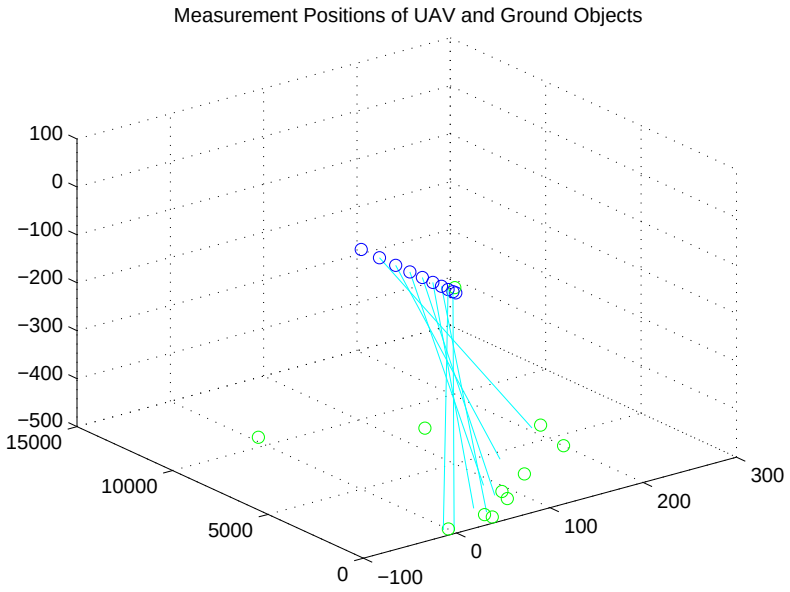

Figure D.1: Scenario 3. Simulated positions of the UAV and ground objects.

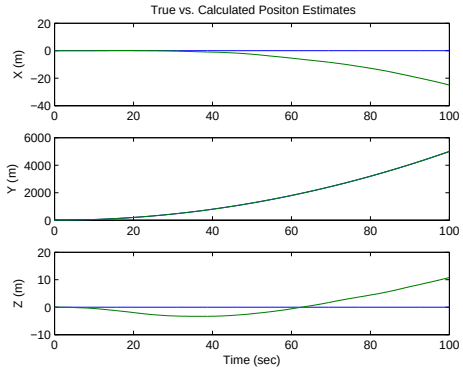

Figure D.2: Scenario 3. True vs calculated position.

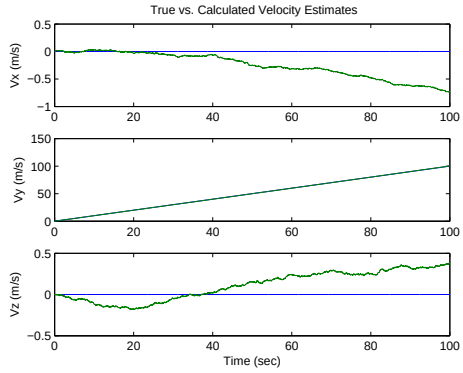

Figure D.3: Scenario 3. True vs calculated velocity.

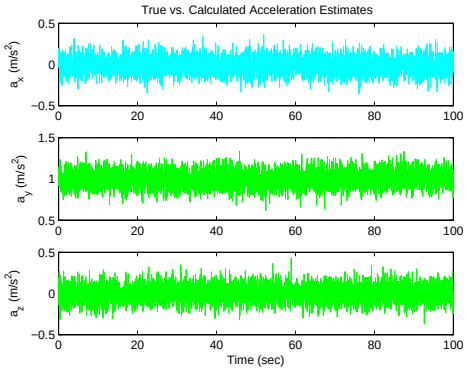

Figure D.4: Scenario 3. True vs calculated acceleration.

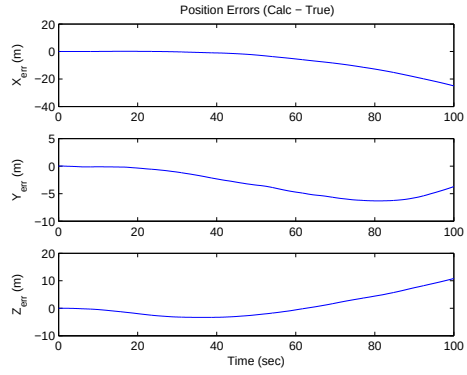

Figure D.5: Scenario 3. Position errors.

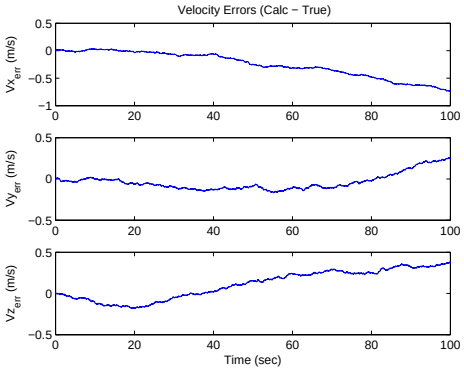

Figure D.6: Scenario 3. Velocity errors.

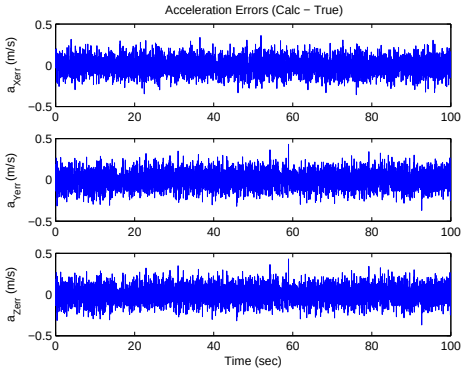

Figure D.7: Scenario 3. Acceleration errors.

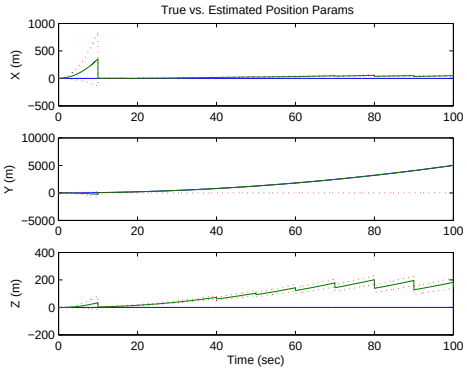

Figure D.8: Scenario 3. Kalman Filter True vs Estimated Position Parameters. Red is +− standart deviation. Blue - true, green -estimated.

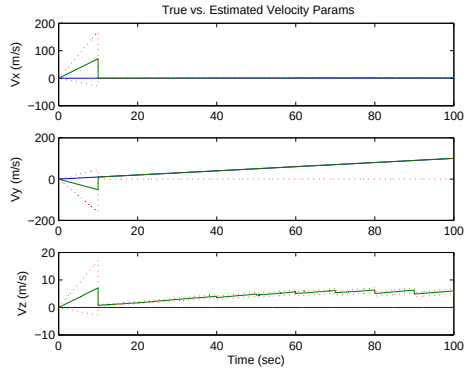

Figure D.9: Scenario 3. Kalman Filter True vs estimated Velocity Parameters. Red is +− standart deviation. Blue - true, green -estimated.

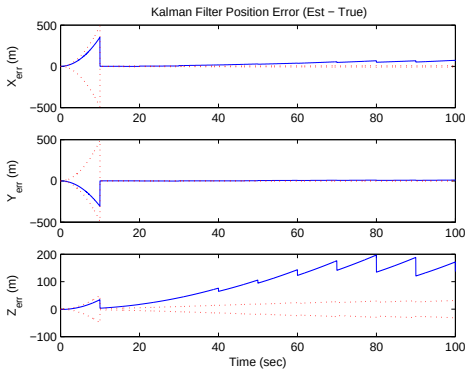

Figure D.10: Scenario 3. Kalman Filter Position Errorts. Estimated - true. Red is +− standart deviation.

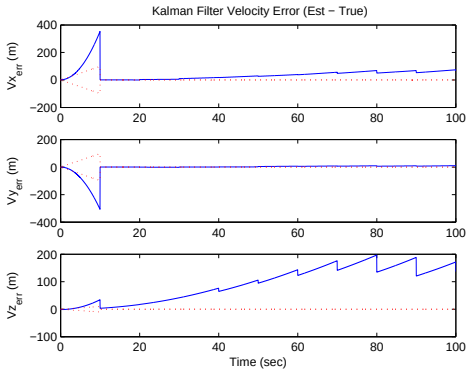

Figure D.11: Scenario 3. Kalman Filter Velocity Errorts. Estimated - true. Red is +− standart deviation.

Appendix E. Plots for Scenario 4

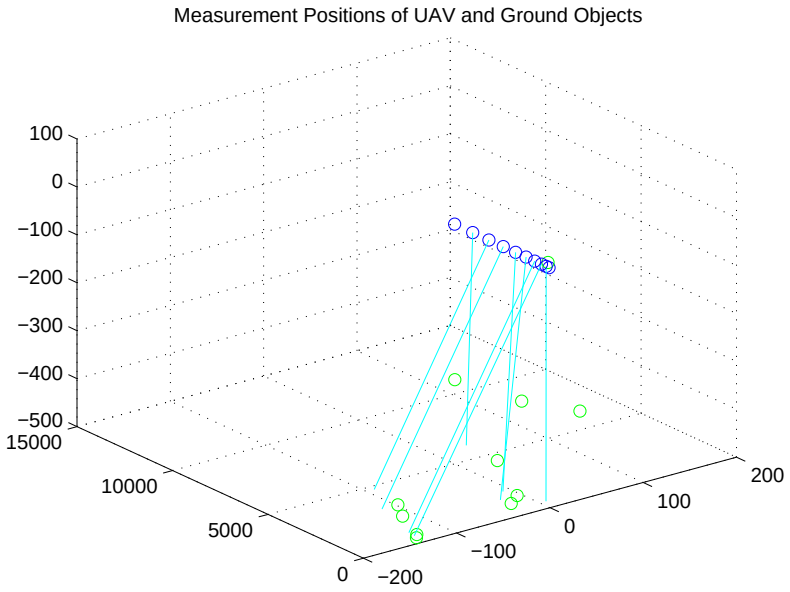

Figure E.1: Scenario 4. Simulated positions of the UAV and ground objects.

E.0.1 True and Calculated Trajectory and Velocity Plots.

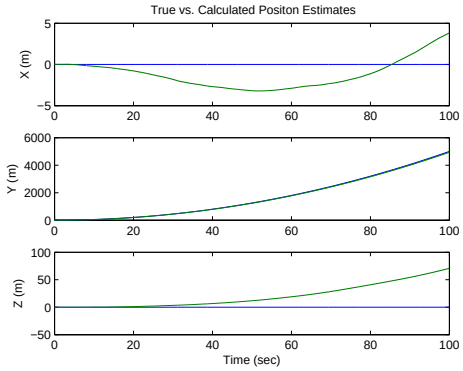

Figure E.2: Scenario 4. True vs calculated position.

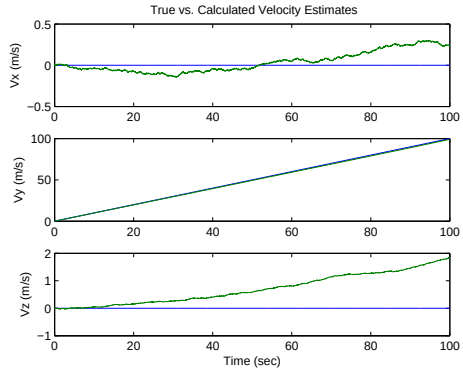

Figure E.3: Scenario 4. True vs calculated velocity.

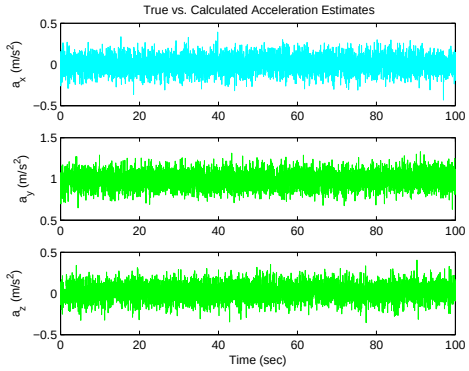

Figure E.4: Scenario 4. True vs calculated acceleration.

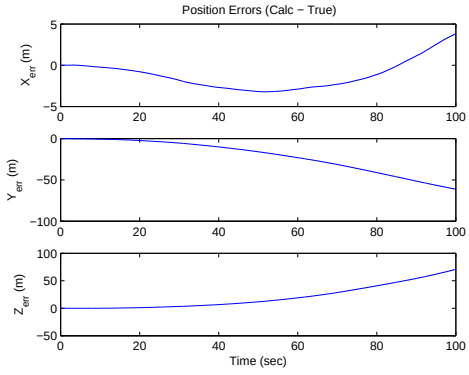

Figure E.5: Scenario 4. Position errors.

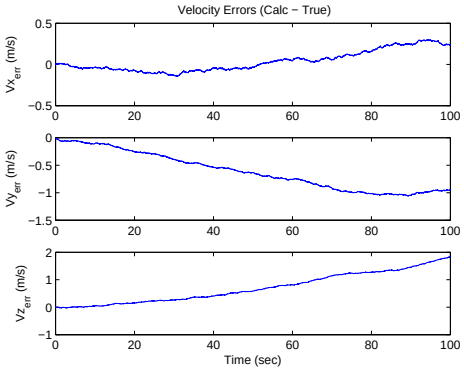

Figure E.6: Scenario 4. Velocity errors.

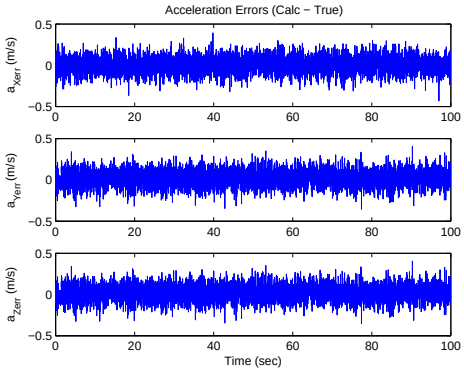

Figure E.7: Scenario 4. Acceleration errors.

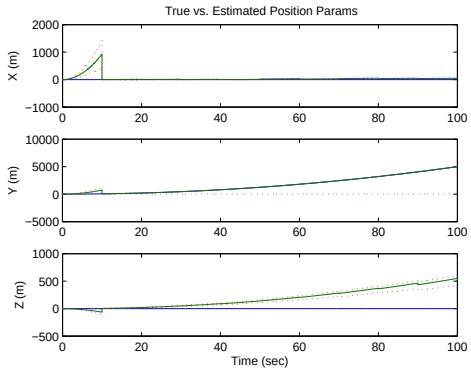

Figure E.8: Scenario 4. Kalman Filter True vs Estimated Position Parameters. Red is +− standart deviation. Blue - true, green -estimated.

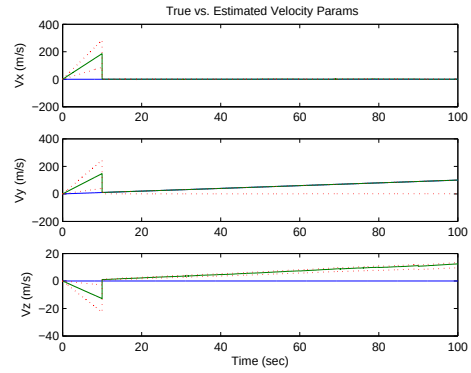

Figure E.9: Scenario 4. Kalman Filter True vs estimated Velocity Parameters. Red is +− standart deviation. Blue - true, green -estimated.

E.0.2 Kalman Filter Results from Perfect Measurement.

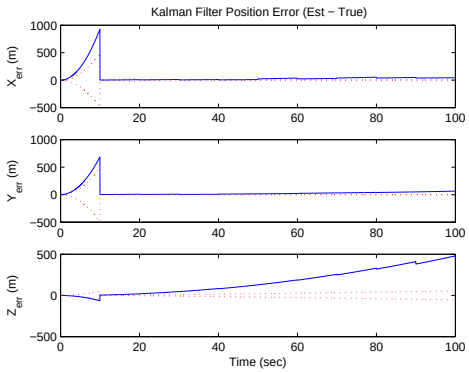

Figure E.10: Scenario 4. Kalman Filter Position Errorts. Estimated - true. Red is +− standart deviation.

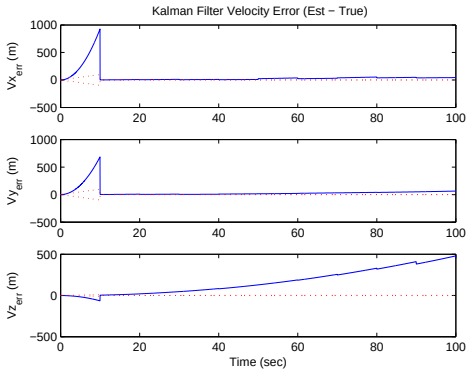

Figure E.11: Scenario 4. Kalman Filter Velocity Errorts. Estimated - true. Red is +− standart deviation.

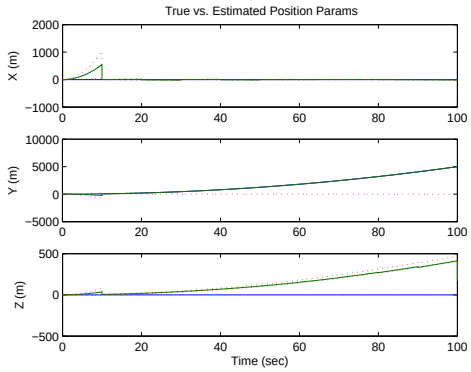

Figure E.12: Scenario 4. Kalman Filter True vs Estimated Position Parameters after Least Square Method Applied. Red is +− standart deviation. Blue - true, green -estimated.

E.0.3 Kalman Filter Results after Least Square Method Applied for Object Geo-Location.

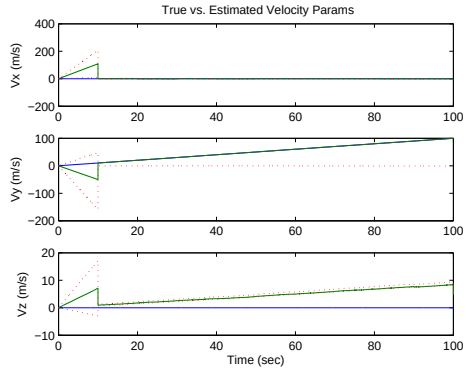

Figure E.13: Scenario 4. Kalman Filter True vs estimated Velocity Parameters after Least Square Method Applied. Red is +− standart deviation. Blue - true, green -estimated.

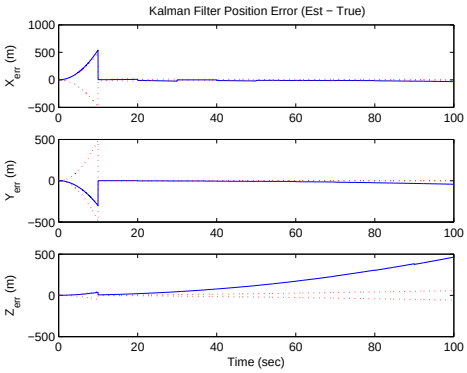

Figure E.14: Scenario 4. Kalman Filter Position Errors after Least Square Method Applied. Estimated - true. Red is +− standart deviation.

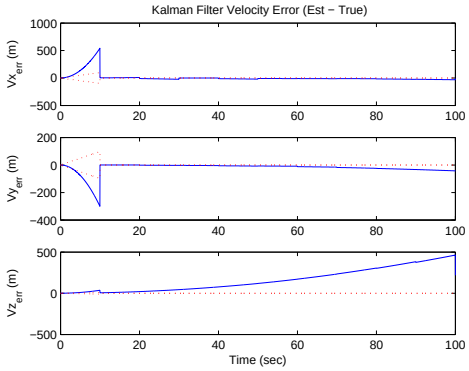

Figure E.15: Scenario 4. Kalman Filter Velocity Errors after Least Square Method Applied. Estimated - true. Red is +− standart deviation.

Bibliography

1. M.Pacher : "INS Aiding by Tracking an Unknown Ground Object - Theory", Proceedings of the 2003 American Control Conference, Denver, CO, June 4-6, 2003.

2. M.Pacher and M.Polat : "Bearing - Only Measurements for INS Aiding: Theory For The Three Dimentional Case", Proceedings of the 2003 AIAA Guidance, Navigation and Control Conference, Austin, Texas, August 11-14, 2003, AIAA paper No 2003-5354.

3. M.Pacher : "Optical Flow for INS Aiding: The 3D Case", Proceedings of the 44th Israel Conference on Aerospace Sciences, Tel Aviv, Israel, February 25-26, 2004.

4. M.Pacher : "Bearing - Only Measurements for INS Aiding: The 3D Case" Proceedings of the American Control Conference, Boston, MA, June 30 - July 2, 2004.

5. M.Pacher : "INS Aiding Using Bearing - Only Measurements of Known Ground Object", Proceedings of the 17th IFAC Symposium on aoutomatic Control in Aerospace, June 25-29 2007, Tulouse, France.

6. M.Pacher, A.Porter and M.Polat : "INS Aiding Using Bearing - Only Measurements of an Unknown Ground Object", ION Journal *Navigation*, Vol. 53, No 1, Spring 2006, pp. 1-20.

7. M.Veth, J.Raquet and M.Pacher : "Stochastic Constraints for Fast Image Correspondance Search with Uncertain Terrain Model", IEEE Trans. on AES, Vol. 42, No. 3, July 2006, pp. 973-982.

8. M.Veth, J.Raquet and M.Pacher : "Correspondance Search Mitigation Using Feature Space Anti-Aliasing", Proceedings of the 63rd Annual Meeting of the Institude of Navigation, Cambridge, MA, April 23-25, 2007.

9. I. Y. Bar-Itzhack and N. Berman: "Control Theoretic Approach to Inertial Navigation Systems", Journal of Guidance, Control and Dynamics, Vol 11, No 3 (1988), pp. 237-245.

10. I. Rhee, M. F. Abdel-Hafez and J. L. Speyer: "Observability of an Integrated GPS/INS During Maneuvers", IEEE Trans. on AES, Vol. 40, No. 2, April 2004, pp. 526-534.

11. M.Nielsen, J.Raquet and M.Pacher : "Development and Flight Test of a Robust Optical - Inertial Navigation System Using Low Cost Sensors", ION GNNS 2008, Savannah, GA, September 16-19, 2008. Reseived *Best Paper* award.

12. R.Brockett : "Finite Dimentional Linear Systems", Wiley, 1970.

REPORT DOCUMENTATION PAGE

Form Approved
OMB No. 0704–0188

1. REPORT DATE *(DD–MM–YYYY)*	2. REPORT TYPE	3. DATES COVERED *(From — To)*
28–08–2009	Master's Thesis	Sept 2007 — Sept 2009

4. TITLE AND SUBTITLE

The Navigation Potential of Ground Feature Tracking

5a. CONTRACT NUMBER

5b. GRANT NUMBER

5c. PROGRAM ELEMENT NUMBER

6. AUTHOR(S)

Mutlu, Guner, Capt., TUAF

5d. PROJECT NUMBER

5e. TASK NUMBER

5f. WORK UNIT NUMBER

7. PERFORMING ORGANIZATION NAME(S) AND ADDRESS(ES)

Air Force Institute of Technology
Graduate School of Engineering and Management (AFIT/EN)
2950 Hobson Way
WPAFB OH 45433-7765

8. PERFORMING ORGANIZATION REPORT NUMBER

AFIT/GE/ENG/09-52

9. SPONSORING / MONITORING AGENCY NAME(S) AND ADDRESS(ES)

Air Force Research Laboratory/ Sensors Directorate
Dr. Stewart DeVilbiss (Tech Advisor)
Reference Systems Brunch, Sensors Directorate
Bldg 620, Rm 3BY57,
2241 Avionics Circle
WPAFB, OH 45433-7303
(Phone: 255-6127x4274 e-mail: Stewart.Devilbiss@wpafb.af.mil)

10. SPONSOR/MONITOR'S ACRONYM(S)

AFRL/RYRN

11. SPONSOR/MONITOR'S REPORT NUMBER(S)

12. DISTRIBUTION / AVAILABILITY STATEMENT

Approval for public release; distribution is unlimited.

13. SUPPLEMENTARY NOTES

14. ABSTRACT

This research effort examines the reduction of error in inertial navigation aided by vision. This is part of an effort focused on navigation in a GPS denied environment. The navigation concept examined here consists of two main steps. First, extract the position of a tracked ground object using vision and geo-locate it in 3 dimensional navigation frame. In this first step multiple positions of the UAV are assumed known; think of a synthetic aperture. The only information about the tracked ground objects/features is the unit vector that points to the objects from the center of the camera. Two such vectors give enough information to calculate the best estimate of the position of the tracked object in a 3 dimensional navigation frame using the method of least square. Concerning the second step: checking observability for the 3-D case shows that at least 2 objects need to be tracked. In practice one needs to track more than two objects to wash out the measurement error and obtain good results.

15. SUBJECT TERMS

viasual aided INS navigation, feature tracking, leasts squares, navigation

16. SECURITY CLASSIFICATION OF:			17. LIMITATION OF ABSTRACT	18. NUMBER OF PAGES	19a. NAME OF RESPONSIBLE PERSON
a. REPORT	b. ABSTRACT	c. THIS PAGE			Dr. Meir Pachter
U	U	U	UU	120	19b. TELEPHONE NUMBER *(include area code)* (937)255-3636 X 7247; Meir.Pachter@afit.edu